Table 1 Clinical details of each patient

Patient no	Age	Sex	Best-corrected visual acuity before treatment (weeks)	Duration (weeks) of symptoms before diagnosis of *Acanthamoeba* keratitis	Immunosuppresion treatment before diagnosis	Culture	Clinical signs				Best-corrected visual acuity after treatment	Follow-up period (months)
							Fungiflora Y	Dendriform epitheliopathy	Radial keratoneuritis	Ring infiltrate		
1	37	Male	20/125	12	Topical steroid	−	+	+	+	−	20/50	12
2	24	Male	20/40	3	−	+	+	−	+	−	20/16	6
3	25	Female	20/40	3	Topical steroid	+	+	−	−	−	20/16	3
4	35	Male	20/32	3	−	+	+	+	+	−	20/16	6
5	18	Female	20/600	2	Topical steroid	+	+	+	+	−	20/25	3
6	25	Female	20/100	3	Topical steroid	−	+	+	+	−	20/16	3
7	25	Female	20/32	1	Topical steroid	+	+	+	+	−	20/16	5
8	33	Male	1f/counting finger	6	Topical steroid	−	+	−	−	+	20/1000	4

When the patients were clinically suspected of having AK, frozen sections of corneal scrapings stained with FFY were made. Under a fluorescence microscope, objects with fluorescent walls were detected (bright green in fig 1C), while the corneal epithelial cells and inflammatory cells did not show the fluorescence (fig 1C). The morphological structure of the corneal epithelium was clearly recognised in the same sections under the light microscope, and the fluorescent spots were identified as *Acanthamoeba* cysts by their morphological appearance (fig 1D).

Acanthamoebic cysts were detected in all eight cases by FFY staining of frozen sections, while five of the eight cases were positive in cultures (table 1). The three cases that showed negative culture results had typical clinical characteristics of AK (table 1).

DISCUSSION

An early diagnosis and appropriate management of AK are critical for ensuring the best visual outcome for patients with AK. We found that frozen sections of corneal scrapings from all of our AK patients stained positively to FFY. Although preparing frozen sections requires some skills, and the examination of the section requires a fluorescence microscope, the procedure for staining with FFY is relatively simple and takes only 15 min. In addition, identifying the cysts requires minimal skills and experience. While most of the special staining procedures for *Acanthamoeba* are time-consuming,[2–5] the entire procedure of FFY staining of frozen sections of corneal scrapings can be accomplished in less than 1 h.

Along with the relatively simple and rapid procedures, another advantage of FFY is that the same sections can be examined by light microscopy because solution A contains haematoxylin, which can be used to visualise acanthamoeba cysts even without eosin. Although FFY was originally developed to detect fungi, the size and morphology of fungi are different from the *Acanthamoeba* cysts and can be easily differentiated. Thus, if a positive staining is detected under the fluorescence microscope, the section can be examined under a light microscope to confirm that the structures have

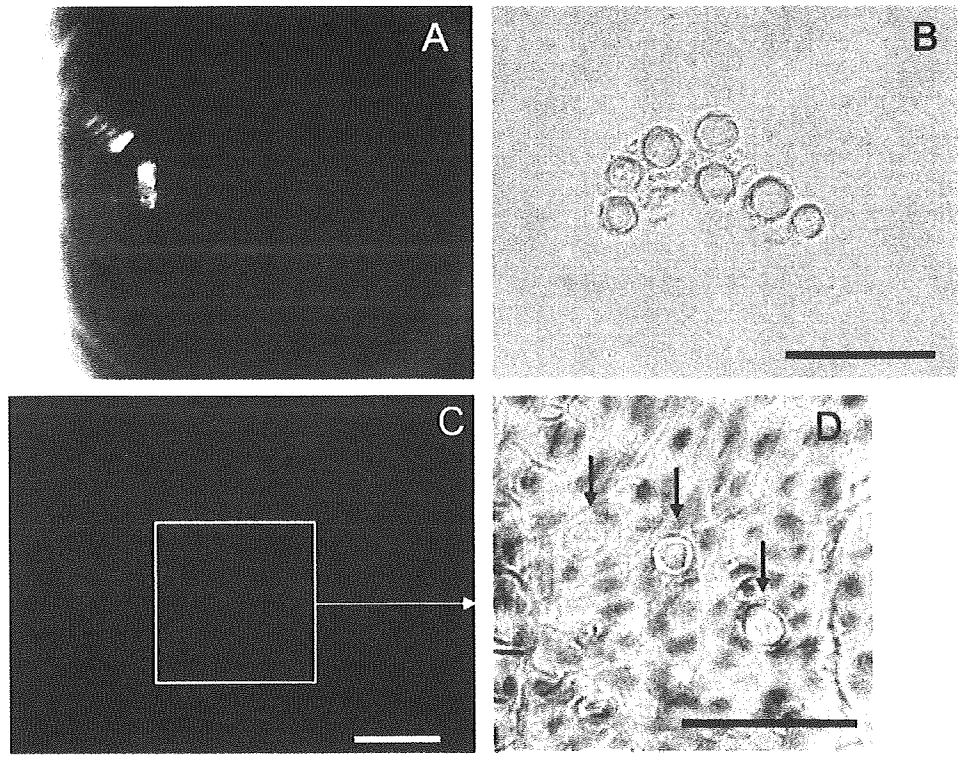

Figure 1 Slit-lamp photograph and histological findings from a patient with *Acanthamoeba* keratitis. (A) Slit-lamp photograph of the cornea of a patient with *Acanthamoeba* keratitis (case 6). Dendriform keratopathy and radial keratoneuritis can be seen. (B) *Acanthamoeba* cysts isolated from the contact lens case of the same patient. (C) FFY staining of frozen sections of corneal scrapings of the same patient showing amebic cysts as bright green circles, while the corneal epithelial cells or inflammatory cells do not fluoresce. (D) Light microscopy showing amoebic cysts in the same section (all bars = 50 μm).

morphological characteristics of acanthamoeba cysts.[5] In this way, false-positive staining can be avoided.

We have used 10 μm serial frozen sections instead of smears which have improved the detection of the *Acanthamoeba* cysts. Importantly, the serial sections maintain the morphology of the corneal epithelium. When corneal epithelial scrapings are prepared as a smear, the morphology and cell forms are easily distorted, and the overlap of structures makes it difficult to detect *Acanthamoeba* cysts. In addition, the entire corneal epithelial scrapings can be prepared into serial frozen sections with this modification. This allows the examiner to examine the entire specimen which will avoid false-negative results.

Impression cytology has already been demonstrated to be useful in diagnosing AK and can be used with FFY staining to improve the accuracy of detection. However, impression cytology has some limitations because it can only examine the surface of the corneal epithelium.[6]

In conclusion, FFY staining of frozen sections of corneal scrapings is an accurate method to detect *Acanthamoeba* cysts. This will improve the ability to detect *Acanthamoeba* cysts at an early stage and should be a useful technique to facilitate early diagnosis of AK.

Competing interests: None.

Ethics approval: Ethics approval was provided by the Institutional Review Board of Ehime University.

Patient consent: Obtained.

Provenance and peer review: Not commissioned; externally peer reviewed.

REFERENCES

1. **Bacon AS,** Frazer DG, Dart JK, *et al.* A review of 72 consecutive cases of *Acanthamoeba* keratitis, 1984–1992. *Eye* 1993;**7**(Pt 6):719–25.
2. **Parmar DN,** Awwad ST, Petroll WM, *et al.* Tandem scanning confocal corneal microscopy in the diagnosis of suspected *Acanthamoeba* keratitis. *Ophthalmology* 2006;**113**:538–47.
3. **Epstein RJ,** Wilson LA, Visvesvara GS, *et al.* Rapid diagnosis of *Acanthamoeba* keratitis from corneal scrapings using indirect fluorescent antibody staining. *Arch Ophthalmol* 1986;**104**:1318–21.
4. **Hahn TW,** O'Brien TP, Sah WJ, *et al.* Acridine orange staining for rapid diagnosis of *Acanthamoeba* keratitis. *Jpn J Ophthalmol* 1998;**42**:108–14.
5. **Silvany RE,** Luckenbach MW, Moore MB. The rapid detection of *Acanthamoeba* in paraffin-embedded sections of corneal tissue with calcofluor white. *Arch Ophthalmol* 1987;**105**:1366–7.
6. **Sawada Y,** Yuan C, Huang AJ. Impression cytology in the diagnosis of *Acanthamoeba* keratitis with surface involvement. *Am J Ophthalmol* 2004;**137**:323–8.
7. **Grossniklaus HE,** Waring GOt, Akor C, *et al.* Evaluation of hematoxylin and eosin and special stains for the detection of *Acanthamoeba* keratitis in penetrating keratoplasties. *Am J Ophthalmol* 2003;**136**:520–6.
8. **Illingworth CD,** Cook SD. *Acanthamoeba* keratitis. *Surv Ophthalmol* 1998;**42**:493–508.
9. **Thomas PA,** Kuriakose T. Rapid detection of *Acanthamoeba* cysts in corneal scrapings by lactophenol cotton blue staining. *Arch Ophthalmol* 1990;**108**:168.
10. **Wilhelmus KR,** Osato MS, Font RL, *et al.* Rapid diagnosis of *Acanthamoeba* keratitis using calcofluor white. *Arch Ophthalmol* 1986;**104**:1309–12.
11. **Inoue T,** Asari S, Tahara K, *et al.* Utility of Fungiflora Y stain in rapid diagnosis of *Acanthamoeba* keratitis. *Br J Ophthalmol* 1999;**83**:632–3.

Molecular Vision 2009; 15:2515-2520 <http://www.molvis.org/molvis/v15/a269>
Received 28 September 2009 | Accepted 25 November 2009 | Published 2 December 2009

Hypoxia-altered signaling pathways of toll-like receptor 4 (TLR4) in human corneal epithelial cells

Yuko Hara,[1] Atsushi Shiraishi,[2,3] Yuichi Ohashi[1,4]

[1]Department of Ophthalmology, Ehime University Graduate School of Medicine, Shitsukawa, Toon, Ehime, Japan; [2]Department of Ophthalmology and Regenerative Medicine, Ehime University Graduate School of Medicine, Shitsukawa, Toon, Ehime, Japan; [3]Department of Cell Growth and Tumor Regulation, Ehime University Graduate School of Medicine, Shitsukawa, Toon, Ehime, Japan; [4]Department of Infectious Diseases, Ehime University Graduate School of Medicine, Shitsukawa, Toon, Ehime, Japan

Purpose: Toll-like receptor 4 (TLR4), a member of the TLR family, is an important pattern recognition molecule that plays a role in the host's innate immune responses to lipopolysaccharide (LPS), a component of gram-negative bacteria. Contact lens wear is one of the risk factors for bacterial keratitis. The purpose of this study was to determine whether hypoxia or contact lens wear alters the TLR4 signaling pathways in human corneal epithelial cells (HCECs).

Method: A simian virus 40-immortalized human corneal epithelial cell (SV40-HCEC) line was cultured under 20% O_2 or 2% O_2 and exposed to LPS. The expression of *TLR4*, interleukin-6 (*IL-6*), and *IL-8* was determined using a real-time reverse transcription-polymerase chain reaction (RT-PCR), enzyme-linked immunosorbent assay (ELISA), and immunoblotting. Immunoblotting was also used to determine whether the nuclear factor kappa B (NFκB) was activated in the SV40-HCEs. HCECs were obtained from 17 healthy volunteers and 18 hydrogel soft contact lens (SCL) wearers using impression cytology (IC), and the expression of the mRNA of *TLR4* was determined using real-time RT-PCR.

Results: A reduction in the expression of the mRNA and protein of TLR4 was detected in SV40-HCECs cultured under hypoxic conditions. Hypoxia also attenuated both the LPS-induced expression of *IL-6* and *IL-8*, and the activation of NFκB in SV40-HCECs. The expression of the mRNA of *TLR4* was down-regulated in the HCECs of soft contact lens wearers.

Conclusions: These results indicate that hypoxia attenuates the TLR4 signaling pathway in HCECs, suggesting that the increase in the susceptibility to bacterial infections under hypoxic conditions may be related to the TLR4 signaling pathways.

Bacterial keratitis is a serious, vision-threatening disease. Until recently, most cases of bacterial keratitis were associated with trauma or ocular surface diseases [1,2]. However, with the increase in the population of contact lens wearers, contact lens wear has become one of the major predisposing factors for microbial keratitis [3-7]. Gram-positive bacteria are the predominant microbiological organisms associated with bacterial keratitis (83% of all positive cultures), and gram-negative bacteria account for only 17% of all bacterial keratitis. However, gram-negative bacteria, mainly *Pseudomonas aeruginosa*, account for 30% of all bacterial keratitis in contact lens wearers [8]. In addition, Bourcier reported that 80.1% of bacterial keratitis cases caused by gram-negative organisms were found in contact lens wearers [8].

It was recently reported that *Pseudomonas aeruginosa* was isolated in 71% of the culture-positive cases of contact lens-related keratitis, and it was the most common isolate in Australia (44.2%) [9].

Correspondence to: Yuko Hara, M.D., Department of Ophthalmology, Ehime University Graduate School of Medicine, Shitsukawa, Toon, Ehime 791-0295, Japan; Phone: 81-89-960-5361; FAX: 81-89-960-5364; email: yukoabc@m.ehime-u.ac.jp

Many pathophysiological effects of contact lens wear have been reported, such as allergic, toxic, mechanical, and osmotic effects. One of the important effects of contact lens wear was the induced hypoxia and hypercapnia of the corneas [10,11].

The corneal epithelial cells are the first line of defense against invading pathogens. One of the mechanisms for this resistance is the antimicrobial components of the tear film, e.g., lactoferrin, lysozyme, mucins, and defensins [12,13].

Recent investigations of the innate immune system have suggested that toll-like receptor systems are involved in the immune system on the ocular surface [14-19].

Toll-like receptors (TLRs) are a family of innate immune-recognizing receptors that recognize the conserved structure of microbes, termed pathogen-associated molecular patterns (PAMPs). TLR4, a member of the TLR family, has been studied extensively in pathogen-mediated host responses, and it functions as a primary detector of lipopolysaccharide (LPS), a component of gram-negative bacteria. Activation of TLR4 induces inflammatory responses by initiating multiple intracellular signaling events, including the activation of nuclear factor kappa B (NF-κB), which ultimately leads to the synthesis and release of many proinflammatory mediators and adhesion molecules, such as interleukin-1 (IL-1), IL-6, IL-8,

TABLE 1. PRIMER PAIRS FOR REAL TIME PCR.

Gene	Forward primer	Reverse primer	Product size (bp): Accession number
IL-6	TACCCCCAGGAGAAGATTCC	TTTTCTGCCAGTGCCTCTTT	175 : M29150
IL-8	GTGCAGTTTTGCCAAGGAGT	CTCTGCACCCAGTTTTCCTT	196 : BC013615
TLR4	TGAGCAGTCGTGCTGGTATC	CAGGGCTTTTCTGAGTCGTC	167 : NM_138554
β-actin	GCACCACACCTTCTACAATGAG	ATAGCACAGCCTGGATAGCAAC	164 : NM_001101

tumor necrosis factor-α (TNF-), and intercellular adhesion molecule 1 (ICAM-1). On the ocular surface, TLR4 with a cluster of differentiation 14 (CD14) and LPS-binding protein (LBP) was reported to induce immune responses against infiltrating gram-negative bacteria [17,20].

The purpose of this study was to determine whether hypoxia is involved in the activation of the TLR 4 signaling systems in human corneal epithelial cells (HCECs), in the LPS-induced expressions of TLR 4, and in the release of inflammatory cytokines as well as activation of NF-κB. To accomplish this, experiments were conducted on a simian virus 40-immortalized human corneal epithelial cell (SV40-HCEC) line under normoxic and hypoxic conditions. We also examined the expression of the mRNA of TLR4 in the HCECs of hydrogel soft contact lens (SCL) wearers.

METHODS

Human subjects: All procedures on human subjects were performed in accordance with the tenets of the principles of the Declaration of Helsinki [21]. The experimental protocol for these experiments was approved by the Institutional Review Board of Ehime University. Informed consent was obtained from all subjects after an explanation of the purpose of the study and the procedures to be used.

Impression cytology (IC): HCECs were collected from 17 healthy volunteers (average age, 34.4±6.4 years) and 18 SCL wearers (average age, 29.9±9.4 years) using impression cytology (IC) with informed consent. Briefly, a drop of 1% oxybuprocaine hydrochloride (Santen, Osaka, Japan) was dropped on the eye, and a 3×5 mm pre-autoclaved nitrocellulose membrane (Millipore, Bedford, MA) was placed on the cornea for 10 s. The membrane was gently removed and placed directly into 350 µl of RLT Buffer (Qiagen, Valencia, CA) for RNA extraction.

Cell cultures: SV40-HCECs were grown to 100% confluence in a supplemented hormonal epithelial medium consisting of Dulbecco's modified eagle medium (DMEM; low glucose)/ F-12 (Invitrogen, Carlsbad, CA), 15% fetal bovine serum (FBS), 10 ng/ml epidermal growth factor, 5 µg/ml insulin, 5 mM L-glutamine, 0.5% dimethyl sulfoxide, and gentamicin [22]. All cells were grown at 37 °C in a humid environment containing 5% CO_2. The cell culture medium was changed every 2 to 3 days.

After the cells reached confluence, the SV40-HCECs were maintained in a keratinocyte serum-free medium (KSFM; Invitrogen) supplemented with 5 ng/ml of human recombinant epidermal growth factor (Invitrogen).

To analyze the effect of oxygen on cell behavior, one group of cells was maintained at 37 °C and 5% CO_2 in a conventional humid tissue culture incubator (20% O_2). A second group of SV40-HCECs was cultured at 37 °C in 5% CO_2 and 2% O_2 using an oxygen monitor to regulate the flow of a calibrated mixture of 95% N_2 and 5% CO_2. After 48 hours, the SV40-HCECs were exposed to 500 ng/ml of recombinant human sCD14 (R&D Systems), 150 ng/ml of recombinant human LBP (R&D Systems), and 100 ng/ml of LPS derived from *Pseudomonas aeruginosa* (Sigma, St. Louise, MO) for 24 h. The SV40-HCECs and the culture supernatant were then collected for further examination.

Real-time reverse transcription-polymerase chain reaction (real-time PCR) analysis: Total RNA was extracted using an RNeasy kit (Qiagen, Valencia, CA) and then reverse-transcribed using Omniscript Reverse Transcriptase (Qiagen) according to the manufacturer's protocols. Real-time PCR was performed with a DyNAmo STBR Green qPCR kit (FINNZYMES, Espoo, Finland) as follows: preheat at 95 °C for 15 min, 40 cycles of denaturation at 95 °C for 10 s, annealing at 60 °C for 20 s, and extension at 72 °C for 30 s using an OPticon2 DNA Engine (BIO RAD, Hercules, CA). The primer pairs used for real-time PCR are listed in Table 1. The C_t values were determined using the Opticon2 software, and the amount of each mRNA was calculated relative to the amount of *β-actin* mRNA in the same samples [23]. Each run was completed with a melting curve analysis in order to confirm the specificity of amplification and lack of primer dimmers.

Enzyme-linked immunosorbent assay (ELISA): The concentrations of IL-6 and IL-8 in the supernatant of the cultured SV40-HCEs were determined with an ELISA test kit (R&D Systems, Minneapolis, MN) following the manufacturer's protocols.

Immunoblotting: Proteins were extracted from the SV40-HCEs using an M-PER mammalian protein extraction reagent (Pierce, Rockford, IL). Each sample (10 µg) was then separated using sodium dodecyl sulfate polyacrylamide gel electrophoresis (SDS-PAGE) under reducing conditions (12% resolving gel) and transferred onto a nitrocellulose membrane (Amersham Biosciences, Piscataway, NJ). The membrane was then blocked for 1 h in 5% dried skim milk in Tris-buffered saline with 0.1% Tween-20 (T-TBS). TLR4 and

NFκB were probed with primary antibodies to NFκB p65 (0.2 μg/ml in 3% bovine serum albumin (BSA) in T-TBS; Santa Cruz Biotechnology, Santa Cruz, CA) or TLR4 (0.2 μg/ml in 3% BSA in T-TBS, BioLegend, San Diego, CA) overnight at 4 °C. The positive immunoreactions were made visible by an enhanced chemiluminescence (ECL plus) detection system (Amersham Pharmacia Biotech). The expression levels of NFκB p65 and TLR4 were determined relative to that of β-actin in the same sample using Quantity one volume analysis (Bio Rad).

Statistical analyses: Each experiment was repeated three times, and representative results are shown in the figures. The values are the means ±standard deviations (SDs). Differences between the groups were tested using a two-tailed paired *t* test. A p-value of <0.05 was considered to be statistically significant.

RESULTS

Hypoxia down-regulated TLR4 expression: To determine whether the expression of TLR4 in SV40-HCECs was altered under hypoxic conditions, SV40-HCEs were cultured under 20% O_2 (control group) or 2% O_2 (hypoxia group) for 48 h. The expression of TLR4 was measured using real-time PCR and immunoblotting. Our results showed that the expression of the mRNA of *TLR4* in the hypoxia group had decreased to about 10% of the control group (Figure 1). Immunoblotting for the expression of the TLR4 protein in the hypoxia group was about 28% of the control group (Figure 2).

Effect of hypoxia on the TLR 4 signaling pathway: To determine whether hypoxic conditions alter the LPS-induced cytokine/chemokines expression in SV40-HCECs, SV40-HCECs were exposed to100 ng/ml of LPS derived from *Pseudomonas aeruginosa* and co-incubated with 500 ng/ml of recombinant human sCD14 and150 ng/ml of recombinant human LBP under 20% O_2 or 2% O_2 for 24 h. The cells and supernatants were collected, and the expressions of the mRNAs of *IL-6* and *IL-8* were evaluated using real-time PCR. The protein levels of IL-6 and IL-8 were determined using ELISA.

Our results showed that the expression of the mRNA of *IL-6* in the hypoxia group had decreased to about 11% of the control group, and the *IL-8* mRNA had also decreased to about 10% of the control group (Figure 3). ELISA showed that the LPS-induced IL-6 production had decreased by about 54% under 20% O_2, and IL-8 had decreased by about 41% under 2% O_2 (Figure 4).

Immunoblotting for NFκB: The effect of hypoxia on the activation of NFκB was determined by immunoblotting 24 h after stimulation by LPS. Immunoblotting showed that the expression of the NFκB protein in the hypoxia group was about 48% of that in the control group (Figure 5).

Expression of TLR4-specific mRNA in human corneal epithelial cells from normal volunteers and SCL wearers: We next examined whether the expression of the mRNA of *TLR4* was altered in the HCECs of SCL wearers. HCECs were collected using IC from SCL wearers and normal volunteers, and then subjected to real-time PCR. The mRNA of *TLR4* was detected in all samples, but the expression level of *TLR4* from the SCL wearers was about one-half of that in normal volunteers (Figure 6).

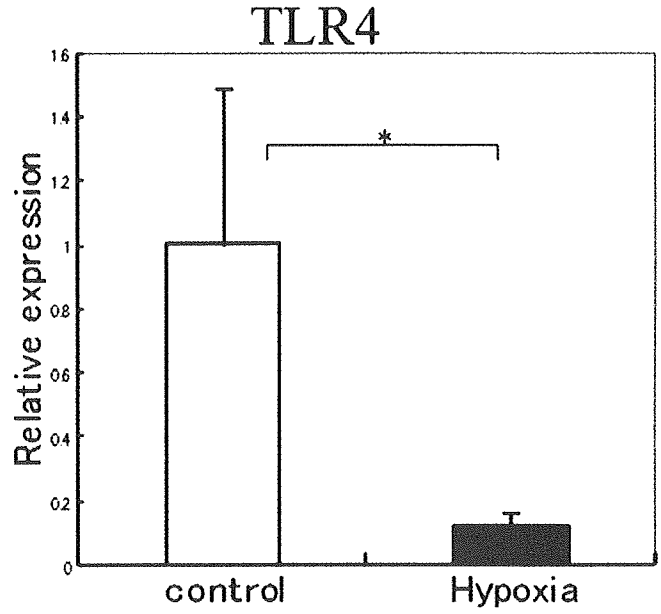

Figure 1. Expression of *TLR4* mRNA in SV40-HCEs cultured under 20% O_2 (control group) or 2% O_2 (hypoxia group). The expression of the mRNA of *TLR4* decreased to about 10% of the control group under hypoxic conditions. The p-values were calculated using two-tailed paired *t* tests. The asterisk indicates a $p<0.05$.

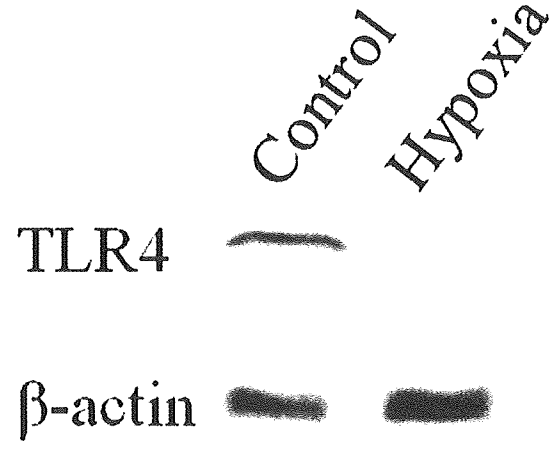

Figure 2. Immunoblotting for TLR4 protein expression in SV40-HCECs cultured under 20% O_2 (control group) or 2% O_2 (hypoxia group). TLR4 protein expression of the hypoxia group decreased to about 30% of the control group.

DISCUSSION

Hypoxia is considered to be one of the main risk factors for bacterial keratitis due to contact lens wear [10,11]. We hypothesized that the altered expression of the mRNA of *TLR4* in HCECs was most likely due to the hypoxia induced by the contact lens wear. Our findings demonstrated that HCECs and SV40-HCECs express the mRNA of *TLR4*, and the level of expression was decreased in SV40-HCECs cultured under hypoxic conditions. We also demonstrated that the expression of *TLR4* mRNA was decreased in the HCECs of SCL wearers. These findings are in agreement with studies reporting that *TLR4* expression was reduced by hypoxia in other type of cells and organs, e.g., cultured pulmonary artery endothelial cells [24]. On the other hand, the mRNA and protein levels of *TLR4* were up-regulated by hypoxia in a cultured microglia cell line [25]. In murine bone marrow-derived dendritic cells, hypoxia did not change the *TLR4* mRNA expression [26]. These different responses of *TLR4* expression under hypoxic conditions may be because of the different hypoxic exposure times in the different experiments. Ock et al. [25] reported that the up-regulation of *TLR4* expression in microglia was observed after 8 h of hypoxic exposure. On the other hand, Ishida et al. [24] reported that long-term (48–72 h) hypoxic exposure caused a down-regulation in the expression of *TLR4* in cultured pulmonary artery endothelial cells. Their results were in good agreement with our results on SV40-HCEs cultured under 2% O_2 for 48 h prior to exposure to LPS. The differences in the types of cells and organs, and in the culture conditions, may account for the different *TLR4* expression. However, the down-regulated expressions of *TLR4* in HCECs under hypoxic conditions are consistent with some of the in vivo and in vitro findings.

We found that the LPS-induced expression of *IL-6* and *IL-8* had decreased and NFκB activation reduced under hypoxia. The TLR4 signaling pathways in corneal epithelial cells have been described, although the conclusions have been controversial. In an in vivo study, the *TLR4* mRNA expression was markedly increased in the cornea of Balb/c mice after infection by *Pseudomonas aeruginosa* [17,18]. On the other hand, there have been reports that the cytokine response induced by activation of TLR4 signaling due to LPS exposure was barely detected in corneal epithelial cells in vitro [14, 15]. In a more recent study, sCD14 and LPS-binding protein (LBP), which are LPS receptor proteins, were identified in

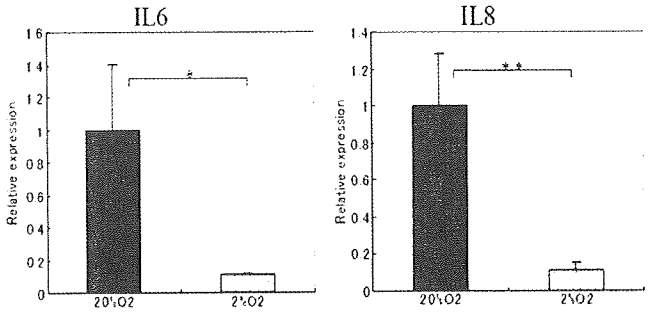

Figure 3. Effects of hypoxia on the expression of cytokines in SV40-HCECs exposed to LPS. Total RNA was isolated from SV40-HCECs cultured under 20% O_2 (control group) or 2% O_2 (Hypoxia group) for 72 h and stimulated with LPS for 24 h. The expression of the mRNA of *IL-6* and *IL-8* was determined using real-time PCR. The relative level of mRNA expression for each cytokine is normalized to *G3PDH* mRNA expression. The p-values were calculated using a two-tailed paired *t* test. The asterisk indicates a $p<0.05$ and the double asterisk indicates a $p<0.01$).

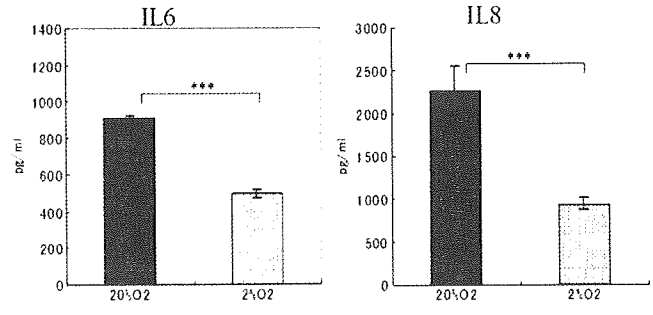

Figure 4. Cytokine secretion by SV40-HCEs cultured under 20% O_2 (control group) or 2% O_2 (hypoxia group) stimulated with LPS. The culture medium was collected 24 h after LPS exposure and analyzed for the presence of IL-6 and IL-8 proteins using ELISA. The p-values were calculated using a two-tailed paired *t* tests. The triple asterisk indicates a $p<0.001$).

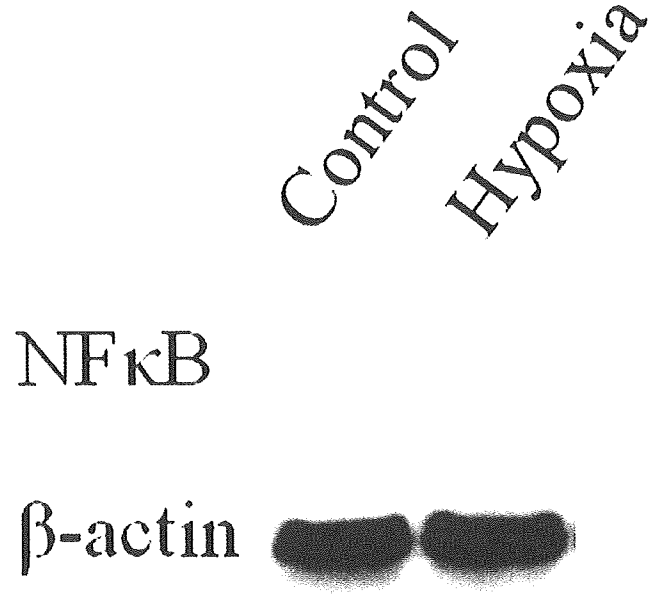

Figure 5. Immunoblotting for NFκB 24 h after exposure to LPS. Immunoblotting showed that NFκB protein expression in the hypoxia group was reduced compared to that in the control group.

human tears and found to mediate the LPS-induced innate immune response by amplifying corneal epithelial cells [20]. In this study, NFκB activation was detected, followed by increased expression of *IL-6* and *IL-8* in SV40-HCECs when stimulated by LPS derived from *Pseudomonas aeruginosa* that was co-incubated with sCD14 and LBP. Our results supported those of Blais et al. [17] and Huang et al. [20], and indicated that the TLR4 signaling systems may play a role in corneal epithelial cells. In our culture system, LPS exposure caused a significant decrease in the mRNA expression of *IL-6* and *IL-8* protein production under hypoxic conditions. In addition, immunoblotting showed that the LPS-induced NFκB activation was also decreased due to hypoxia. Thus, hypoxia attenuated not only the *TLR4* expression, but also the LPS-induced TLR 4 signaling pathways.

It has been demonstrated that hypoxia activates many transcriptional factors, including NFκB [27,28]. Our findings are in contrast to those reported earlier. However, we investigated the effects of hypoxia on the LPS-induced NFκB activation or cytokine production, whereas the earlier studies investigated the effect of hypoxia on NFκB activation only. It has been reported that hypoxia up-regulated *TLR4* mRNA expression and enhanced the IRF-3 pathway, whereas it decreased the LPS-induced NFκB pathways in microglial cells [25]. Recently, it was reported that cigarette smoke causing hypoxia reduced *TLR4* mRNA and LPS responsiveness, and severe chronic obstructive pulmonary disease (COPD) had a more significant association with reduced *TLR4* expression than less severe disease [29]. The expression of *TLR4* may have important implications for inflammation and infection in response to pathogens.

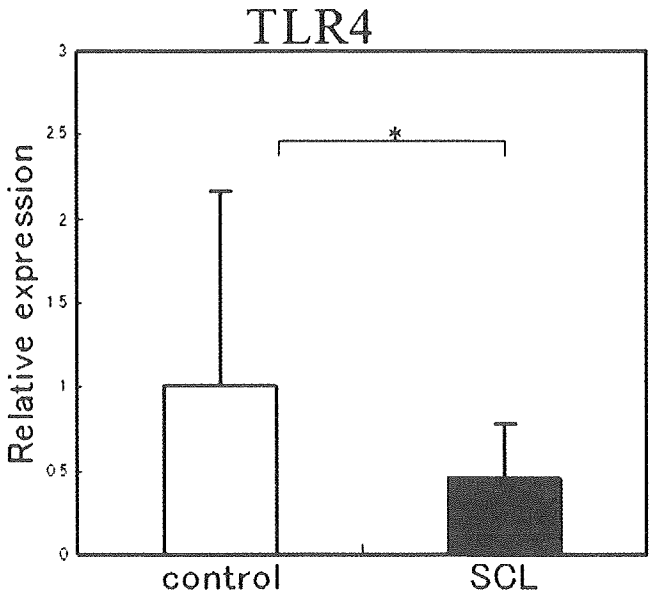

Figure 6. Expression of *TLR4* mRNA in the CECs of normal volunteers and SCL wearers. *TLR4* mRNA was detected from all samples, but the expression of *TLR4* from SCL wearers was one-half the amount from normal volunteers. The p-values were calculated using a two-tailed paired *t* test. The asterisk indicates a $p<0.05$.

Thus, NFκB activation and cytokine production are regulated complex interactions. It may be possible that hypoxia decreased the LPS-induced NFκB activation in the TLR4 signaling pathway, although there are some differences in duration, hypoxic exposure, and the use of different types of cells.

In conclusion, the expression of *TLR4* was decreased in the HCECs of SCL wearers and SV40-HCECs under hypoxic conditions. In addition, hypoxia decreased the LPS-induced expression of *IL-6* and *IL-8* as well as the activation of NFκB in SV40-HCECs. These results indicate that the contact lens-induced hypoxia may increase the susceptibility to bacterial infections such as *Pseudomonas aeruginosa* by altering the TLR4 signaling pathways.

ACKNOWLEDGMENTS

This work was supported by a Grant-in-Aid for Young Scientists (B) 19791273 from the Ministry of Education, Culture, Sports, Science, and Technology of Japan.

REFERENCES

1. Musch DC, Sugar A, Meyer RF. Demographic and predisposing factors in corneal ulceration. Arch Ophthalmol 1983; 101:1545-8. [PMID: 6626005]
2. Benson WH, Lanier JD. Current diagnosis and treatment of corneal ulcers. Curr Opin Ophthalmol 1998; 9:45-9. [PMID: 10387468]
3. Dart JK. Predisposing factors in microbial keratitis: the significance of contact lens wear. Br J Ophthalmol 1988; 72:926-30. [PMID: 3147696]
4. Liesegang TJ. Contact lens-related microbial keratitis: Part I: Epidemiology. Cornea 1997; 16:125-31. [PMID: 9071523]
5. Cheng KH, Leung SL, Hoekman HW, Beekhuis WH, Mulder PG, Geerards AJ, Kijlstra A. Incidence of contact-lens-associated microbial keratitis and its related morbidity. Lancet 1999; 354:181-5. [PMID: 10421298]
6. Keay L, Edwards K, Brian G, Naduvilath T, Stapleton F. Evaluation of surveillance methods for an epidemiological study of contact lens related microbial keratitis. Clin Experiment Ophthalmol 2004; 32:349-53. [PMID: 15281965]
7. Stapleton F, Keay L, Edwards K, Naduvilath T, Brian G, Jacobs R. Studies of contact lens-related microbial keratitis in Australia and New Zealand: new learnings. Eye Contact Lens 2007; 33:354-7. [PMID: 17975419]
8. Bourcier T, Thomas F, Borderie V, Chaumeil C, Laroche L. Bacterial keratitis: predisposing factors, clinical and microbiological review of 300 cases. Br J Ophthalmol 2003; 87:834-8. [PMID: 12812878]
9. Green M, Apel A, Stapleton F. Risk factors and causative organisms in microbial keratitis. Cornea 2008; 27:22-7. [PMID: 18245962]
10. Liesegang TJ. Contact lens-related microbial keratitis: Part II. Pathophysiology. Cornea 1997; 16:265-73. [PMID: 9143796]

11. Ichijima H, Hayashi T, Mitsunaga S, Hamano H. Determination of oxygen tension on rabbit corneas under contact lenses. CLAO J 1998; 24:220-6. [PMID: 9800061]
12. Davidson HJ, Kuonen VJ. The tear film and ocular mucins. Vet Ophthalmol 2004; 7:71-7. [PMID: 14982585]
13. McNamara NA, Andika R, Kwong M, Sack RA, Fleiszig SM. Interaction of Pseudomonas aeruginosa with human tear fluid components. Curr Eye Res 2005; 30:517-25. [PMID: 16020285]
14. Song PI, Abraham TA, Park Y, Zivony AS, Harten B, Edelhauser HF, Ward SL, Armstrong CA, Ansel JC. The expression of functional LPS receptor proteins CD14 and toll-like receptor 4 in human corneal cells. Invest Ophthalmol Vis Sci 2001; 42:2867-77. [PMID: 11687531]
15. Ueta M, Nochi T, Jang MH, Park EJ, Igarashi O, Hino A, Kawasaki S, Shikina T, Hiroi T, Kinoshita S, Kiyono H. Intracellularly expressed TLR2s and TLR4s contribution to an immunosilent environment at the ocular mucosal epithelium. J Immunol 2004; 173:3337-47. [PMID: 15322197]
16. Ueta M, Hamuro J, Kiyono H, Kinoshita S. Triggering of TLR3 by polyI:C in human corneal epithelial cells to induce inflammatory cytokines. Biochem Biophys Res Commun 2005; 331:285-94. [PMID: 15845391]
17. Huang X, Du W, McClellan SA, Barrett RP, Hazlett LD. TLR4 Is Required for Host Resistance in Pseudomonas aeruginosa Keratitis. Invest Ophthalmol Vis Sci 2006; 47:4910-6. [PMID: 17065506]
18. Huang X, Hazlett LD, Du W, Barrett RP. SIGIRR promotes resistance against Pseudomonas aeruginosa keratitis by down-regulating type-1 immunity and IL-1R1 and TLR4 signaling. J Immunol 2006; 177:548-56. [PMID: 16785552]
19. Hara Y, Shiraishi A, Kobayashi T, Kadota Y, Shirakata Y, Hashimoto K, Ohashi Y. Alteration of TLR3 pathways by glucocorticoids may be responsible for immunosusceptibility of human corneal epithelial cells to viral infections. Mol Vis 2009; 15:937-48. [PMID: 19452017]
20. Blais DR, Vascotto SG, Griffith M, Altosaar I. LBP and CD14 secreted in tears by the lacrimal glands modulate the LPS response of corneal epithelial cells. Invest Ophthalmol Vis Sci 2005; 46:4235-44. [PMID: 16249503]
21. World Medical Association declaration of Helsinki. Recommendations guiding physicians in biomedical research involving human subjects. JAMA 1997; 277:925-6. [PMID: 9062334]
22. Araki-Sasaki K, Ohashi Y, Sasabe T, Hayashi K, Watanabe H, Tano Y, Handa H. An SV40-immortalized human corneal epithelial cell line and its characterization. Invest Ophthalmol Vis Sci 1995; 36:614-21. [PMID: 7534282]
23. Rutledge RG, Cote C. Mathematics of quantitative kinetic PCR and the application of standard curves. Nucleic Acids Res 2003; 31:e93. [PMID: 12907745]
24. Ishida I, Kubo H, Suzuki S, Suzuki T, Akashi S, Inoue K, Maeda S, Kikuchi H, Sasaki H, Kondo T. Hypoxia diminishes toll-like receptor 4 expression through reactive oxygen species generated by mitochondria in endothelial cells. J Immunol 2002; 169:2069-75. [PMID: 12165534]
25. Ock J, Jeong J, Choi WS, Lee WH, Kim SH, Kim IK, Suk K. Regulation of Toll-like receptor 4 expression and its signaling by hypoxia in cultured microglia. J Neurosci Res 2007; 85:1989-95. [PMID: 17461416]
26. Kuhlicke J, Frick JS, Morote-Garcia JC, Rosenberger P, Eltzschig HK. Hypoxia Inducible Factor (HIF)-1 Coordinates Induction of Toll-Like Receptors TLR2 and TLR6 during Hypoxia. PLoS One 2007; 2:e1364. [PMID: 18159247]
27. Murdoch C, Muthana M, Lewis CE. Hypoxia regulates macrophage functions in inflammation. J Immunol 2005; 175:6257-63. [PMID: 16272275]
28. Cummins EP, Taylor CT. Hypoxia-responsive transcription factors. Pflugers Arch 2005; 450:363-71. [PMID: 16007431]
29. MacRedmond RE, Greene CM, Dorscheid DR, McElvaney NG, O'Neill SJ. Epithelial expression of TLR4 is modulated in COPD and by steroids, salmeterol and cigarette smoke. Respir Res 2007; 8:84. [PMID: 18034897]

The print version of this article was created on 28 November 2009. This reflects all typographical corrections and errata to the article through that date. Details of any changes may be found in the online version of the article.

Molecular Vision 2009; 15:1589-1593 <http://www.molvis.org/molvis/v15/a169>
Received 6 July 2009 | Accepted 11 August 2009 | Published 14 August 2009

New technique for culturing corneal epithelial cells of normal mice

Takeshi Kobayashi,[1] Ryuji Yoshioka,[2] Atsushi Shiraishi,[1,3] Yuichi Ohashi[2]

[1]Department of Ophthalmology and Regenerative Medicine, Ehime University School of Medicine, Shitsukawa, Toon, Ehime, Japan; [2]Department of Ophthalmology, Ehime University School of Medicine, Shitsukawa, Toon, Ehime, Japan; [3]Department of Cell Growth and Tumor Regulation, Ehime University School of Medicine, Shitsukawa, Toon, Ehime, Japan

Purpose: To describe a new method of culturing mouse corneal epithelial cells (MCECs).
Methods: MCECs were isolated from C57/BL6 mouse corneas and cultured on type-I collagen-coated plastic dishes in low-calcium progenitor cell targeting medium (CnT-50). Expression of the mRNAs of N-terminal truncated isoform of p63 (*DNp63*), cytokeratin 12 (*K12*), and cytokeratin 14 (*K14*) were determined by reverse transcription-polymerase chain reaction (RT-PCR). To examine the differentiation capabilities, passage 3 (P3) MCECs at confluence were subcultured on amniotic membrane (AM) in a differentiation medium (CnT-30) until confluence. At confluence, 1 mM calcium was added and cultured for 4 more days. The expression of K12 in the stratified MCECs was analyzed by immunostaining.
Results: The MCECs cultured in CnT-50 proliferated until at least P10. The number of cells at confluency at P3 was 61.8 (SD ±9.4, n=5) times that at P0. MCECs cultured on AM in CnT-30 with addition of calcium were stratified up to two to three layers, and the stratified MCECs expressed K12. *DNp63* mRNA was continuously expressed throughout the different passages, and *K12* mRNA was detected in P0 cells and the stratified MCECs on AM.
Conclusions: Cultured MCECs maintain their proliferation and differentiation capabilities as well as their corneal epithelial cell characteristics. These results suggest that MCECs produced by this culturing method provide a useful experimental model which can enable further development of research of the corneal epithelium.

Mice are used in many different types of studies for several reasons: they are well-suited for genetic manipulations such as genomic sequence analyses; different strains with different characteristics are readily available, and many transgenic (Tg) and knockout strains have been created and are commercially available. Furthermore, in vitro approaches with cultured mouse cells allow the investigation of tissue or cell specific properties.

To investigate the physiological and pathological conditions of corneal epithelial cells, many corneal epithelial cell lines and primary culture systems have been established for humans and rabbits [1-6]. However, there have been few reports regarding the creation of a corneal epithelial cell line and primary culture system for mice.

Hazlett et al. [7] developed a method for short-term cultures of primary mouse corneal epithelial cells (MCECs), although they failed to subculture the cells past passage three, and the cultures may have been contaminated by fibroblasts. Since then, some researchers reported on the results of in vitro examinations of primary MCECs, and they were able to study these cells without any effect from adjacent tissue cells and matrices [8,9]. Unfortunately, a large number of eyes were used to obtain sufficient number of cells for the primary cultures, and the culture conditions were not stable among the different experimental groups.

Recently, Kawakita et al. [10] and Ma et al. [11] demonstrated that long-term cultures of MCECs could be achieved by culturing MCECs in keratinocyte serum-free medium. Although their technique required several weeks to establish a stable cell line and the probability of the establishment was 55%, there was a possibility that their method could establish a MCEC line. However, there was still some concern on whether the cells in this cell line maintained corneal properties, e.g., expression of ketratin 12.

Because it is important to have sufficient number of MCECs to perform reproducible experiments and to reduce the number of experimental animals used, it is necessary to develop an easily repeatable method to culture and grow MCECs that maintain the properties of normal MCECs. Thus, the purpose of this study was to develop a simple and reproducible method for culturing MCECs that will allow the cells to retain their proliferation and differentiation capabilities. To accomplish this, we used a low-calcium, low-bovine pituitary extract (BPE), serum-free progenitor cell targeted medium to culture MCECs.

METHODS

Tissue preparation and cell culture: C57/BL6 mice (CLEA Japan Inc, Tokyo, Japan), aged 4-8 weeks, were handled in accordance with the guidelines in the ARVO Statement for the Use of Animals in Ophthalmic and Vision Research. Intact and viable MCEC sheets were prepared as described with

Correspondence to: Atsushi Shiraishi, Department of Ophthalmology and Regenerative Medicine, Ehime University School of Medicine, Shitsukawa, Toon, Ehime 791-0295, Japan; Phone: 81-89-960-5361; FAX: 81-89-960-5364; email: shiraia@m.ehime-u.ac.jp

TABLE 1. PCR PRIMERS USED IN THIS STUDY

Target	Primer	Primer sequence	Amplicon length	GenBank accession
K12	Forward	ACTAGAGCCGACCTGGAAGC	158	NM_010661
	Reverse	ACCTTGGTGAGATCCACTCC		
K14	Forward	ACCGCAAGGATGCTGAGGA*	103	NM_016958
	Reverse	GAAATCTCACTCTTGCCGCTCTG*		
DNp63	Forward	CTGGAAAACAATGCCCAGACTCA	126	AF075437
	Reverse	TGCGTGGTCTGTGTTGTAGG		AF075438
				AF075439
ß-actin	Forward	CATCCGTAAAGACCTCTATGCCAAC*	171	NM_007393
	Reverse	ATGGAGCCACCGATCCACA*		

The asterisk indicates that the primer sequences for K14 and ß-actin were designed by Takara Bio Inc. (Otsu, Japan).

some modifications [11]. In brief, the eyes were enucleated from the euthanized animals and incubated in DMEM/F12 (1:1 mixture; Invitrogen, Tokyo, Japan) containing 15 mg/ml dispase II (Roche Diagnostics, Basel, Switzerland), 100 mM sorbitol, and antibiotic-antimycotic (1X; Invitrogen) for 18 h at 4 °C. The loosened corneal epithelial sheets were peeled off with forceps and incubated in 100 µl of 0.25% trypsin (Invitrogen) for 10 min at 37 °C. To inhibit the activity of trypsin, 100 µl of 2 mg/ml soybean trypsin inhibitor (Roche Diagnostics) in PBS(-) was added to the medium, and the sheets were separated into single cells by pipetting. Then 2 ml of low-calcium, low- bovine pituitary extract (BPE), serum-free progenitor cell targeted medium (CnT-50; CELLnTEC, Bern, Switzerland) or low-calcium, serum- and BPE-free progenitor cell targeted medium (CnT-20; CELLnTEC) was added to the isolated cells. The cells were then transferred to type-I collagen coated 35 mm plastic dishes (Asahi Techno Glass, Funabashi, Japan). The cultures were incubated at 37 °C under 95% humidity and 5% CO_2. The medium was changed every 2 to 3 days. Confluent cultures of MCECs were subcultured at a density 1×10^4 cells/cm^2.

Preparation of cultured corneal epithelial cell sheets: To examine the differentiation potential of the MCECs, confluent cells at passage 3 (P3) were subcultured on amniotic membrane (AM) in low-calcium, serum- and BPE-free differentiation medium (CnT-30; CELLnTEC). When the cells had reached confluency, the medium (CnT-30) was changed to CnT-30 supplemented with calcium (1 mM) and the medium was changed daily for 4 days. The MCEC sheets on the AM were collected.

RNA extraction and reverse transcription-polymerase chain reaction (RT-PCR): For RNA extraction, the epithelial surface of normal 4-week-old C57/BL6 mouse corneas were scraped with a scalpel, and the epidermal layer was excised with scissors. Total RNA was extracted from normal mouse corneal epithelia (MCE) and normal mice epidermal (MED) tissue, and also from MCEC sheets, and MCECs harvested from confluent primary culture (P0) and P3 with RNeasy Mini kit (Qiagen, Tokyo, Japan). cDNAs were made by reverse transcription of the total RNA with the SuperScript VILO cDNA Synthesis Kit (Invitrogen) according to the manufacturer's protocol.

PCR was performed with AmpliTaq Gold PCR Master Mix (Applied Biosystems, Tokyo, Japan) in 20 µl containing 2 µl of cDNA, 0.25 µM concentrations of primer, and 10 µl of the 2X PCR Master Mix. The mixture was subjected to 30 cycles of 15 s at 95 °C for denaturation, 30 s at 60° C for primer annealing and extension. The PCR primers are listed in Table 1.

Immunohistochemical analyses: MCEC sheets were fixed in 4% paraformaldehyde/phosphate-buffered saline (PBS) at 4 °C. After fixation and dehydration in a graded series of ethanol, the samples were embedded in paraffin and cut into 5 µm sections. The sections were blocked in a solution containing 2% rabbit serum, 2% BSA, and 0.1% Triton-X 100 in PBS for 1 h, followed by incubation with 0.2 mg/ml of goat anti-cytokeratin 12 (Santa Cruz Biotechnology, Inc. Santa Cruz, CA) in CanGetSignal A (TOYOBO, Osaka, Japan) overnight at 4 °C. Immunoreactivity to primary antibodies was made visible by secondary antibody conjugated with FITC (Vector Laboratories, Burlingame, CA). After rinsing in PBS, the sections were mounted on glass slides with ProLong Gold Antifade Reagent with DAPI (Invitrogen).

RESULTS

Characteristics of cultured MCECs: Mouse corneal epithelial cells (MCECs), which were cultured on type-I collagen coated plastic dishes in low calcium, low BPE, serum-free medium (CnT-50), continued to proliferate until at least P10. The MCECs had a cobble stone-like appearance which did not change throughout the 10 passages (Figure 1A-C).

The MCECs in low-calcium, serum- and BPE-free medium (CnT-20) were also able to proliferation until at least P3 (Figure 1D), but the rate of proliferation of MCECs in

CnT-20 was considerably slower than in CnT-50 (data not shown). The proliferation curve of MCECs in CnT-50 is shown in Figure 2, and each value was the mean of five experiments. The number of cells was counted at confluence of each passage, and was normalized to the value at P0. The means±standard deviations of cells at P1, P2, and P3 were 6.7±5.2 (n=5) times, 16.7±3.6 (n=5) times, and 61.8±9.4 (n=5) times that at P0. The interval from primary cell seeding to confluence of P3 ranged from 24 to 52 days.

RT-PCR: DNp63, *K12*, and *K14* mRNA expression was detected in normal mouse cornea, and *DNp63* and *K14* but not *K12* were detected in normal mouse epidermis (Figure 3). The expression of *DNp63* and *K14* mRNA was detected in cells from P0 and P3 of MCECs and MCEC sheets, while the expression of *K12* mRNA was detected in MCECs at P0 and MCEC sheets but not at P3 (Figure 3).

Differentiation potential of cultured MCEs: MCECs were subcultured on AM in serum- and BPE-free differentiation medium (CnT-30) supplemented with 1 mM of calcium. The cells proliferated and were stratified to two to three layers by four days (Figure 4A). Immunoreactivity to K12, a corneal epithelium specific differentiation marker, was detected in the stratified MCECs as seen in normal mouse corneal epithelia (Figure 4B,D). The MCEC sheets did not stain with nonspecific goat IgG (Figure 4C).

DISCUSSION

Our results demonstrated that a simple culture method can maintain MCECs up to P10. The MCECs were cultured on type-I collagen-coated plastic dishes in low-calcium serum-free medium, which is commercially available. The MCECs maintained their proliferation and differentiation capabilities, and had corneal epithelial cell characteristics.

Low-calcium, serum-free, or no BPE human corneal epithelial progenitor cell targeted (PCT) media (CnT-50 or CnT-20) have been used for isolation and proliferation studies of early passage human CECs [12,13]. Although the number of studies using these media has been limited, the PCT media appears to be effective for culturing human CECs. Because we were not aware of any studies using the PCT medium for MCECs, we have examined its effectiveness for MCECs. We found that the MCECs cultured in CnT-50 continued to

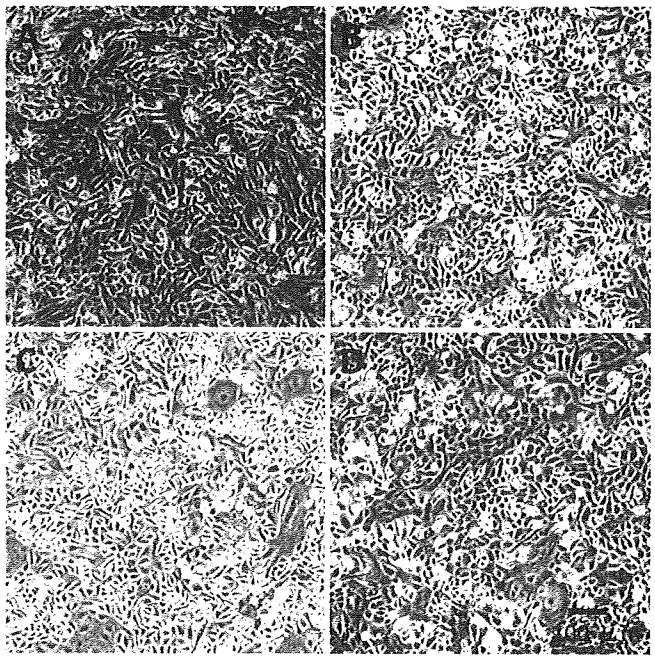

Figure 1. Phase contrast photomicrographs of mouse corneal epithelial cells (MCECs). MCECs at confluence in CnT-50 medium at different passages; **A**, passage 0 (P0); **B**, P3, and **C**, P10. MCECs at confluency at P3 cultured in CnT20 (**D**). Scale bar; 100 μm.

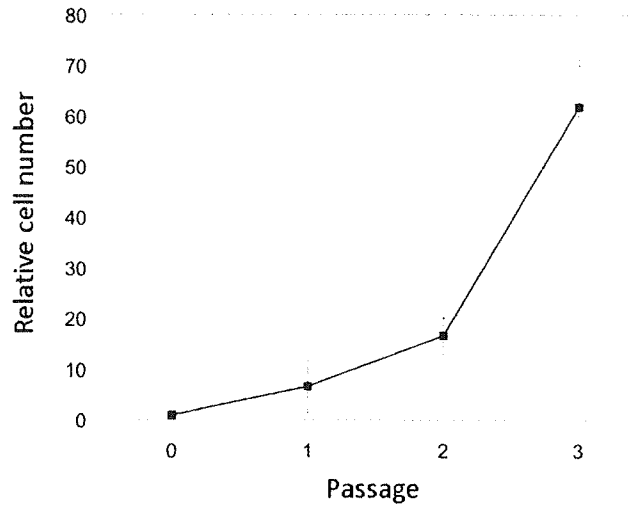

Figure 2. Growth of MCECs cultured in CnT-50. Each point is the mean of five individual experiments. The number of cells at confluency at each passage was counted and normalized to the number at P0. Error bar represents the standard deviations.

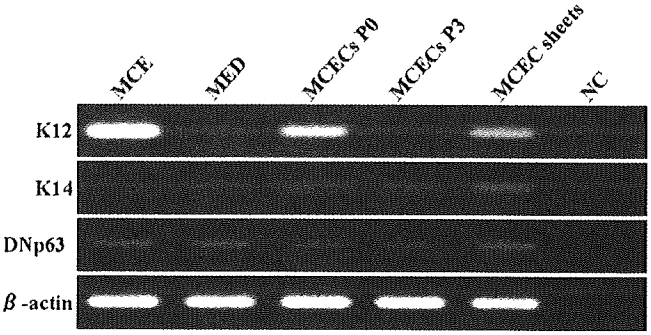

Figure 3. *K12*, *K14*, and *DNp63* mRNA expression. *K12*, *K14*, and *DNp63* mRNA expression in normal mouse corneal epithelia (MCE), normal mouse epidermis (MED), MCECs at confluence at P0 and P3, and MCEC sheets. PCR products were analyzed by 1.5% agarose gel electrophoresis. PCRs with no DNA template were used as negative control (NC).

proliferate until at least P10, and the morphology of the cells was not altered throughout the ten passages (Figure 1). A relatively faster rate of proliferation was observed in a medium containing low concentrations of BPE (CnT-50) than in a complete defined medium (CnT-20), although the morphology of the cells was not different (Figure 1).

Recently, Kawakita, et al. [11] and Ma, et al. [10] reported on methods for culturing MCECs, however, it required several weeks to establish a stable cell line of MCECs, and the probability of the establishing the cell line was 55%. On the other hand, we attempted to culture MCECs five times by our method, and were successful each time. Our analyses showed that the MCECs had proliferated to 61.8 times (ranged from 54.5 to 76.9) that at P0 within the three passages (Figure 2).

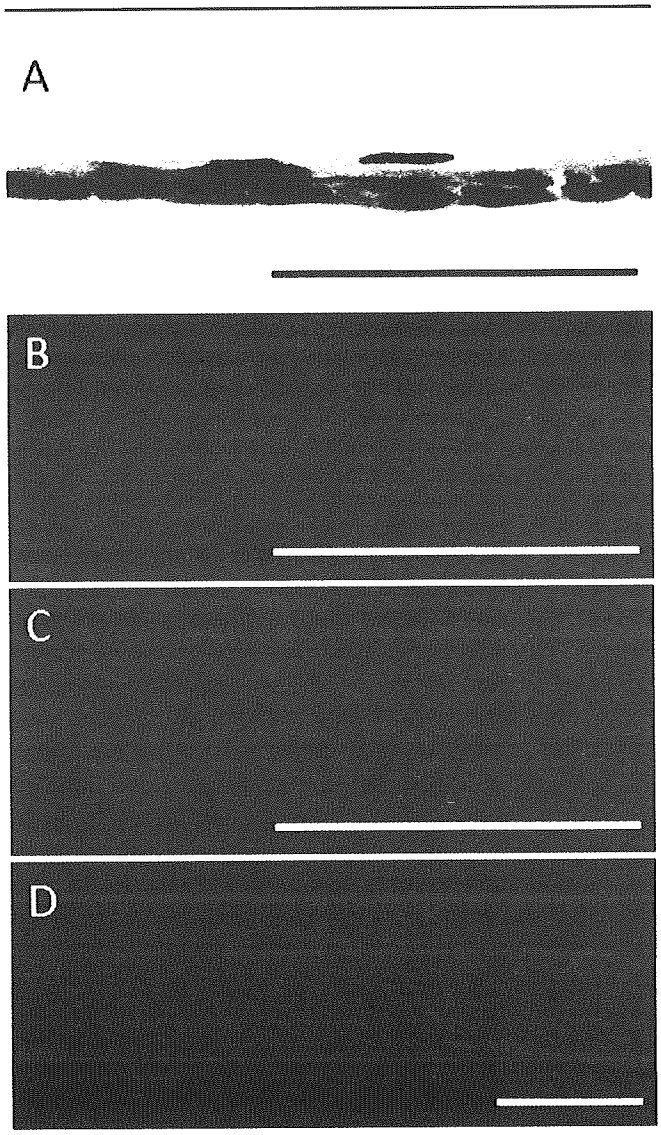

Figure 4. Immunohistochemical staining of MCEC sheets. Paraffin sections (5 μm) were stained with; **A** = H&E, **B** = immunostained with anti-cytokeratin 12, and **C** = normal goat IgG. Normal mouse cornea was immunostained with anti-cytokeratin 12 (**D**). Scale bar; 50 μm.

In the cultured MCECs, the expression of *DNp63* mRNA was detected throughout the passages examined (Figure 3). DNp63 is known to be a transcription factor that is essential for the differentiation of progenitor stratified squamous epithelial cells, e.g., corneal epithelial cells and epidermal cells [14,15]. During the differentiation of stratified squamous epithelial cells, DNp63 is expressed in the basal cells, but not in differentiated cells [14,15]. These results suggest that the differentiation capability was well maintained in MCECs cultured in CnT-50.

It has been recognized that multiple passaged cultured cells may alter their cellular properties. Indeed at P3, the MCECs cultured in CnT-50 did not express *K12* mRNA. Therefore, we next examined whether the MCECs maintain the corneal epithelial characteristics as well as the differentiation potential. Confluent P3 MCECs cultured on AM in differentiation medium (CnT-30) supplemented with 1 mM calcium expressed *K12* and were stratified up to two to three layers. Ma et al. [10] also demonstrated the differentiation potential and *K12* expression in cultured MCECs, however they failed to detect *K12* expression at the protein level. On the other hand, our immunohistochemical results clearly showed positive staining of K12 in the stratified MCECs grown on AM as seen in normal mouse cornea. It is well recognized that AMs provide a better microenvironment for corneal epithelial cells, and it has been reported that the use of AM promotes the corneal epithelial cell differentiation [16-18]. Thus, the expression of *K12* might be better with the AM, however MCECs cultured in CnT-50 still maintain the corneal epithelial characteristics after P3.

Our analyses also showed that the MCECs proliferated an average of 61.8 times more (range: 54.5 - 76.9) at P3 than at P0 (Figure 2). When cells were collected from ten mouse eyes and cultured to confluence in CnT-50, the number of cells reached 3.0×10^7 by the third passage. This number is more than sufficient for most in vitro experiments.

In conclusion, a commercially available low-calcium, low-BPE, serum-free medium (CnT-50) made it possible to grow MCECs on type-I collagen coated plastic dishes. The relatively simple and reproducible results of culturing MCECs with CnT-50 should be valuable for laboratory experiments.

ACKNOWLEDGMENTS

The authors would like to acknowledge a Grant-in-Aid for Scientific Research (C) 20592079 from the Ministry of Education, Culture, Sports, Science, and Technology of Japan.

REFERENCES

1. Araki-Sasaki K, Ohashi Y, Sasabe T, Hayashi K, Watanabe H, Tano Y, Handa H. An SV40-immortalized human corneal

epithelial cell line and its characterization. Invest Ophthalmol Vis Sci 1995; 36:614-21. [PMID: 7534282]

2. Adhikary G, Crish J, Lass J, Eckert RL. Regulation of involucrin expression in normal human corneal epithelial cells: a role for activator protein one. Invest Ophthalmol Vis Sci 2004; 45:1080-7. [PMID: 15037572]
3. Dey S, Patel J, Anand BS, Jain-Vakkalagadda B, Kaliki P, Pal D, Ganapathy V, Mitra AK. Molecular evidence and functional expression of P-glycoprotein (MDR1) in human and rabbit cornea and corneal epithelial cell lines. Invest Ophthalmol Vis Sci 2003; 44:2909-18. [PMID: 12824231]
4. Esco MA, Hazlett LD, Kurpakus-Wheater M. Pseudomonas aeruginosa binds to extracellular matrix deposited by human corneal epithelial cells. Invest Ophthalmol Vis Sci 2002; 43:3654-9. [PMID: 12454032]
5. Morita S, Shirakata Y, Shiraishi A, Kadota Y, Hashimoto K, Higashiyama S, Ohashi Y. Human corneal epithelial cell proliferation by epiregulin and its cross-induction by other EGF family members. Mol Vis 2007; 13:2119-28. [PMID: 18079685]
6. O'Brien WJ, Krema C, Heimann T, Zhao H. Expression of NADPH oxidase in rabbit corneal epithelial and stromal cells in culture. Invest Ophthalmol Vis Sci 2006; 47:853-63. [PMID: 16505017]
7. Hazlett L, Masinick S, Mezger B, Barrett R, Kurpakus M, Garrett M. Ultrastructural, immunohistological and biochemical characterization of cultured mouse corneal epithelial cells. Ophthalmic Res 1996; 28:50-6. [PMID: 8726677]
8. Ramaesh T, Ramaesh K, Leask R, Springbett A, Riley SC, Dhillon B, West JD. Increased apoptosis and abnormal wound-healing responses in the heterozygous Pax6+/- mouse cornea. Invest Ophthalmol Vis Sci 2006; 47:1911-7. [PMID: 16638998]
9. Levin MH, Verkman AS. Aquaporin-3-dependent cell migration and proliferation during corneal re-epithelialization. Invest Ophthalmol Vis Sci 2006; 47:4365-72. [PMID: 17003427]
10. Ma X, Shimmura S, Miyashita H, Yoshida S, Kubota M, Kawakita T, Tsubota K. Long-term culture and growth kinetics of murine corneal epithelial cells expanded from single corneas. Invest Ophthalmol Vis Sci 2009; 50:2716-21. [PMID: 19218612]
11. Kawakita T, Espana EM, He H, Yeh LK, Liu CY, Tseng SC. Calcium-induced abnormal epidermal-like differentiation in cultures of mouse corneal-limbal epithelial cells. Invest Ophthalmol Vis Sci 2004; 45:3507-12. [PMID: 15452056]
12. Qi H, Li DQ, Bian F, Chuang EY, Jones DB, Pflugfelder SC. Expression of glial cell-derived neurotrophic factor and its receptor in the stem-cell-containing human limbal epithelium. Br J Ophthalmol 2008; 92:1269-74. [PMID: 18723744]
13. Qi H, Li DQ, Shine HD, Chen Z, Yoon KC, Jones DB, Pflugfelder SC. Nerve growth factor and its receptor TrkA serve as potential markers for human corneal epithelial progenitor cells. Exp Eye Res 2008; 86:34-40. [PMID: 17980361]
14. Blanpain C, Fuchs E. p63: revving up epithelial stem-cell potential. Nat Cell Biol 2007; 9:731-3. [PMID: 17603506]
15. Di Iorio E, Barbaro V, Ruzza A, Ponzin D, Pellegrini G, De Luca M. Isoforms of DeltaNp63 and the migration of ocular limbal cells in human corneal regeneration. Proc Natl Acad Sci USA 2005; 102:9523-8. [PMID: 15983386]
16. Grueterich M, Espana E, Tseng SC. Connexin 43 expression and proliferation of human limbal epithelium on intact and denuded amniotic membrane. Invest Ophthalmol Vis Sci 2002; 43:63-71. [PMID: 11773014]
17. Grueterich M, Espana EM, Tseng SC. Modulation of keratin and connexin expression in limbal epithelium expanded on denuded amniotic membrane with and without a 3T3 fibroblast feeder layer. Invest Ophthalmol Vis Sci 2003; 44:4230-6. [PMID: 14507866]
18. Koizumi N, Fullwood NJ, Bairaktaris G, Inatomi T, Kinoshita S, Quantock AJ. Cultivation of corneal epithelial cells on intact and denuded human amniotic membrane. Invest Ophthalmol Vis Sci 2000; 41:2506-13. [PMID: 10937561]

The print version of this article was created on 11 August 2009. This reflects all typographical corrections and errata to the article through that date. Details of any changes may be found in the online version of the article.

Molecular Vision 2009; 15:937-948 <http://www.molvis.org/molvis/v15/a98>
Received 24 February 2009 | Accepted 23 April 2009 | Published 8 May 2009

Alteration of TLR3 pathways by glucocorticoids may be responsible for immunosusceptibility of human corneal epithelial cells to viral infections

Yuko Hara,[1] Atsushi Shiraishi,[2] Takeshi Kobayashi,[2] Yuko Kadota,[1] Yuji Shirakata,[3] Koji Hashimoto,[3] Yuichi Ohashi[1]

[1]Department of Ophthalmology, Ehime University School of Medicine, Shitsukawa, Japan; [2]Department of Ophthalmology and Regenerative Medicine, Ehime University School of Medicine, Shitsukawa, Japan; [3]Department of Dermatology, Ehime University School of Medicine, Shitsukawa, Japan

Purpose: The toll-like receptor 3 (TLR3) recognizes viral double-stranded RNA and its synthetic analog polyriboinosinic-polyribocytidylic acid (poly(I:C)), and the activation of TLR3 is known to induce the production of type I interferon (IFN) and inflammatory cytokines/chemokines. The purpose of this study was to determine the role played by innate responses to a herpes simplex virus 1 (HSV-1) infection of the corneal epithelial cells. In addition, we determined the effects of immunosuppressive drugs on the innate responses.Methods: Cultured human corneal epithelial cells (HCECs) were exposed to poly(I:C), and the expressions of the mRNAs of the cytokines/chemokines macrophage-inflammatory protein 1 alpha (*MIP1-α*), macrophage-inflammatory protein 1 beta (*MIP1-β*), interleukin-6 (*IL-6*), interleukin-8 (*IL-8*), regulated on activation, normal T cell expressed and secreted (*RANTES*), Interferon-beta (*IFN-β*), and *TLR3* were determined using real-time reverse transcription-polymerase chain reaction (RT-PCR). The effects of dexamethasone (DEX, 10^{-6} or 10^{-5} M) and cyclosporine A (CsA, 10^{-6} or 10^{-5} M) on the expression of these cytokines and *TLR3* were also determined using real-time RT-PCR. Levels of MIP1-α, MIP1-β, IL-6, IL-8, RANTES, and IFN-β were measured using the enzyme-linked immunosorbent assay (ELISA). The activation of nuclear factor kappa B (NFκB) and interferon regulatory factor 3 (IRF3) in HCECs was assessed by immunohistochemical staining. The effects of DEX and CsA on HCECs exposed to HSV-1 (McKrae strain) were also examined.Results: The expressions of *MIP1-α*, *MIP1-β*, *IL-6*, *IL-8*, *RANTES*, *IFN-β*, and *TLR3* were up-regulated in HCECs exposed to poly(I:C). The poly(I:C)-induced expressions of *IL-6* and *IL-8* were down-regulated by both DEX and CsA, while the expressions of *IFN-β* and *TLR3* were suppressed by DEX alone. Similarly, the poly(I:C)-induced activation of NFκB was decreased by both DEX and CsA, and the activation of IRF3 was reduced by DEX alone. When HCECs were inoculated with HSV-1, DEX led to a decrease in the expression of *IL6*, *IFN-β*, and *TLR3*, and an extension of plaque formation.Conclusion: These results indicate that DEX may increase the susceptibility of HCECs to viral infections by altering the TLR3 signaling pathways.

The toll-like receptors (TLRs) are a family of innate immune receptors that recognize the conserved structures of microbes, termed pathogen-associated molecular patterns (PAMPs). The TLR system has been extensively studied in immune cells, e.g. in macrophages, and recent studies have demonstrated that epithelial cells also express TLRs. Thus, respiratory epithelial cells express TLR 1–10 [1,2], epidermal keratinocytes express TLR1, 2, 4, and 5 [3,4], intestinal epithelial cells express TLR1–4, 6, and 9 [5], and female reproductive tract epithelial cells express TLR1–9 [6]. In the eye, human corneal epithelial cells express TLR 1–7, 9, and 10 [7], and human conjunctival epithelial cells express TLR 1–6 and 9 [8].

The question then arises whether the TLRs play a role in the keratitis caused by the herpes simplex virus (HSV). It is known that treatment of stromal keratitis with topical acyclovir significantly reduces the number of patients who suffer serious visual impairment. However, keratitis often recurs in immunocompromised hosts or in individuals who receive steroid therapy for a long period of time. In fact, topical or systemic application of glucocorticoids results in the reactivation of herpes keratitis [9,10], and glucocorticoids are contraindicated for epithelial keratitis because they can worsen the clinical course to virus-induced geographic keratitis [11].

Recent studies have shown that a TLR3 ligand, which is a double-stranded RNA (dsRNA) can activate different types of epithelial cells, e.g. airway epithelial cells, female reproductive tract epithelial cells, and corneal epithelia cells [7,12,13]. TLR3 is the only TLR that does not interact with myeloid differentiation factor 88 (MyD88) as a signaling adaptor [14]. TLR3 interacts directly with the adaptor protein, Toll/interleukin-1 receptor (TIR) domain-containing adaptor inducing IFN-β (TRIF), which is also called the TIR-

Correspondence to: Yuko Hara, Department of Ophthalmology, Ehime University School of Medicine Shitsukawa, Toon, Ehime 791-0295, Japan; Phone: 81-89-960-5361; FAX: 81-89-960-5364; email: yukoabc@m.ehime-u.ac.jp

Table 1. Primer pairs for real-time PCR.

Gene	Forward primer	Reverse primer	Product size (bp:Accession number)
IL-6	TACCCCCAGGAGAAGATTCC	TTTTCTGCCAGTGCCTCTTT	175 : M29150
IL-8	GTGCAGTTTTGCCAAGGAGT	CTCTGCACCCAGTTTTCCTT	196 : BC013615
MIP-1α	TGCAACCAGTTCTCTGCATC	TTTCTGGACCCACTCCTCAC	198 : BC071834
MIP-1β	AAGCTCTGCGTGACTGTCCT	GCTTGCTTCTTTTGGTTTGG	211 : NM_002984
IFN-β	CATTACCTGAAGGCCAAGGA	CAGCATCTGCTGGTTGAAGA	178 : V00534
RANTES	GAGGCTTCCCCTCACTATCC	CTCAAGTGATCCACCCACCT	155 : BC008600
TLR3	AGCCTTCAACGACTGATGCT	TTTCCAGAGCCGTGCTAAGT	201 : NM_003265
G3PDH	CGACCACTTTGTCAAGCTCA	AGGGGAGATTCAGTGTGGTG	203 : BT006893

containing adaptor molecule (TICAM-1). TRIF/TICAM-1 activates the transcription factor NFκB and the interferon regulatory factor 3 (IRF3) [15,16]. The activation of NFκB leads to the production of inflammatory cytokines/ chemokines, and the activation of IRF3 elicits anti-viral responses, especially through the production of type I IFN [15,17,18]. The production of type I IFN is the first line of defense against viral infections, and it acts by limiting the early replication of viruses [19,20]. Deonarain et al. [21] demonstrated that IFN-β is crucial for this process, because IFN-β-deficient mice are highly susceptible to viral infections.

TLR3 recognizes dsRNA and would not be expected to detect DNA from a DNA virus, such as HSV. However, it is known that most viruses synthesize dsRNA during their replication [22], and therefore TLR3 should be able to recognize HSV. Recently, Kariko et al. [23] reported that TLR3 is stimulated by cellular mRNA, and Ashkar et al. [24] reported that the delivery of ligands for TLR3, but not TLR4, protected against HSV-2 infections. Hayashi et al. [25] reported that herpes simplex virus 1 (HSV-1) elicited inflammatory cytokines via TLR3 and TLR9 in the corneal epithelial cells. Thus, corneal epithelial cells may play a role as the first line of defense against viral infection, including HSV infection, through the TLRs.

The purpose of this study was to determine the role played by innate responses in controlling HSV-1 infection of the corneal epithelial cells. In addition, we examined whether immunosuppressive drugs altered the HSV-1 infection of the cornea. We shall show that polyriboinosinic-polyribocytidylic acid (poly(I:C)), a TLR3 agonist, can induce anti-viral responses in corneal epithelial cells. However, these anti-viral responses can be altered by dexamethasone (DEX) and cyclosporine A (CsA).

METHODS

Human subjects: All procedures on human subjects conformed to the tenets of the Declaration of Helsinki [26]. The experimental protocol for these experiments was approved by the Institutional Review Board of Ehime University.

Chemicals and cell cultures: All reagents used for the cell cultures were purchased from Invirogen (Carlsbad, CA). Primary human corneal epithelial cells (HCECs) were isolated from human corneoscleral buttons dissected from eyes acquired from an American Eye Bank(Sight Life Seattle WA) as reported [27]. Briefly, the buttons were carefully denuded of the endothelial cells and adherent iris. After digestion with 1.2 U/ml dispase at 4 °C for 24 h, the loosened epithelial sheets were removed and dispersed into single cells by enzyme digestion with 0.1% trypsin and 0.02% EDTA. Then, the HCECs were cultured in serum-free modified MCDB 153 type II medium, supplemented with insulin (5 μg/ml), hydrocortisone (5×10^{-7} M), ethanolamine (0.1 mM), phosphoethanolamine (0.1 mM), Insulin-like growth factor-1 (IFG-1; 10 ng/ml), Epidermal growth factor (EGF; 0.1 ng/ml), and Ca^{2+} (0.06 mM). The medium was changed every 2 days.

To determine the effects of DEX and CsA on the poly(I:C)-induced expression of cytokines/chemokines, HCECs were cultured with hydrocortisone-free, modified MCDB 153 type II medium for 24 h, then incubated with 100 ng/ml of poly(I:C) in the presence or absence of DEX (10^{-6} or 10^{-5} M) or CsA (10^{-6} or 10^{-5} M). In the CsA control, CsA was substituted with 0.01% dimethyl sulfoxide (DMSO), which was also used to reconstitute the CsA. After 24 h of stimulation the cells and supernatants were collected.

Real-time PCR analysis: Total RNA was extracted from the cultured HCECs using RNeasy kit (Qiagen, Valencia, CA), and then reverse-transcribed using Omniscript Reverse Transcriptase (Qiagen) according to the manufacturer's protocols. Real-time PCR was performed with the DyNAmo SYBR Green qPCR Kit (Finnzymes, Espoo, Finland) as follows: 95 °C for 15 min; 40 cycles of denaturation at 95 °C for 10 s; annealing at 60 °C for 20 s; and extension at 72 °C for 30 s using the OPticon 2 DNA Engine (BioRad, Hercules, CA). The primer pairs used for real-time PCR are listed in Table 1. The C_t values were determined by the Opticon 2 software, and the amount of each mRNA was calculated relative to the amount of Glyceraldehyde 3 phosphate dehydrogenase (*GAPDH*) mRNA in the same samples [28]. Each run was completed with a melting curve analysis to confirm the specificity of the amplification and the absence of primer dimers.

Measurement of proinflammatory cytokines/chemokines production: The concentrations of MIP1-α, MIP1-β, IL-6,

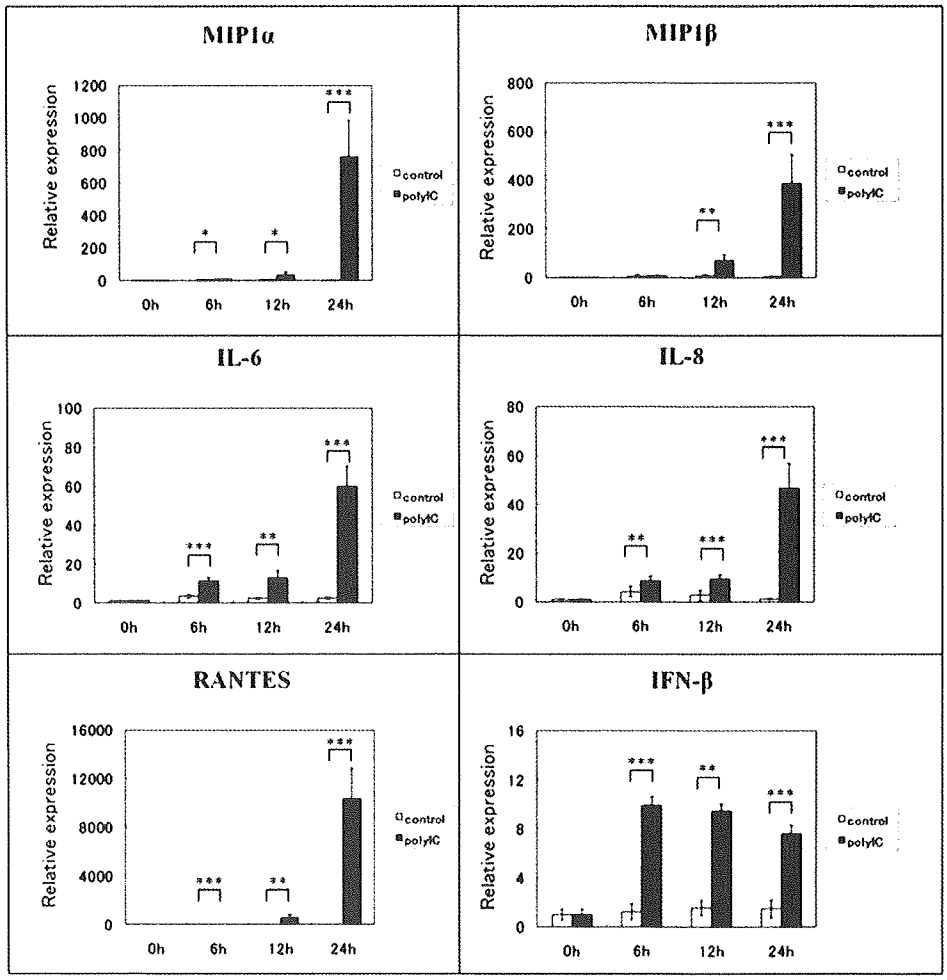

Figure 1. Expression of the mRNAs of cytokines and chemokines by HCEs exposed to poly(I:C), a TLR3 ligand. Total RNA was isolated from HCECs at 6, 12, and 24 h after poly(I:C) exposure, and the expressions of the mRNAs of *MIP1-α*, *MIP1-β*, *IL-6*, *IL-8*, *RANTES*, and *IFN-β* were determined by real-time PCR. The relative level of expression of each cytokine and chemokine mRNA is normalized to the level of *G3PDH* mRNA expression. The p values were calculated using two-tailed paired t-tests, (*p<0.05, **p<0.01, ***p<0.001).

IL-8, RANTES, and IFN-β in the supernatants of the cultured HCECs were determined using an ELISA kit (R&D Systems, Minneapolis, MN) following the manufacturer's protocols.

Immunostaining for NFκB and IRF3: HCECs were cultured on CultureSlides (BD Falcon, Bedford, MA) with 100 ng/ml of poly(I:C) in the presence or absence of DEX (10^{-5} M) or CsA (10^{-5} M) for 3 h. Cells were washed three times with phosphate-buffered saline (PBS), then fixed for 15 min in 3.2% paraformaldehyde (PFA)/PB. After washing with PBS, cells were permeabilized with 0.1% Triton X-100 for 5 min, followed by incubation with primary antibodies to NFκB p65 (0.2 μg/ml; Santa Cruz Biotechnology, Santa Cruz, CA) or to IRF3 (0.2 μg/ml; Santa Cruz Biotechnology) in 1% bovine serum albumin (BSA)/PBS at 4 °C for 16 h. After washing with PBS, the slides were incubated with specific secondary antibodies, then incubated with appropriate fluorescein (FITC) conjugated antibodies (Pierce, Rockford, IL). Finally, the slides were coverslipped using an anti-fading mounting medium (Vector, Burlingame, CA). For the controls, sections were treated with normal rabbit immunoglobulin G (IgG), and no positive staining was detected with any of the antibodies.

Herpes simplex virus 1 (HSV-1) infection: Stocks of the McKrae strain of HSV-1 were propagated on African green monkey kidney (Vero) cells grown in complete Dulbecco's modified Eagle's medium (DMEM) containing 10% fetal bovine serum (FBS), 1% penicillin, and streptomycin. The titer of virus stocks was determined by the standard plaque assay on Vero cells, and titers were expressed as plaque-forming units (PFU)/ml. Stocks were stored at –70 °C in 1 ml aliquots, and a fresh aliquot of stock virus was used for each experiment.

HCECs were cultured in a hydrocortisone-free, modified MCDB 153 type II medium for 24 h, and cultured in the presence or absence of DEX (10^{-5} M) or CsA (10^{-5} M) prior to exposure to HSV-1. For the plaque assay, HCECs were inoculated with HSV-1 at a multiplicity of infection (MOI) of 50 for 48 h, and the cells were then fixed with 10% formalin and stained with crystal violet. The area of the plaques was measured by Adobe Photoshop software (Adobe Systems Incorporated, San Jose, CA) to evaluate the efficiency of infection. The supernatants were also collected to evaluate the concentration of HSV-1 DNA by real-time PCR. To examine

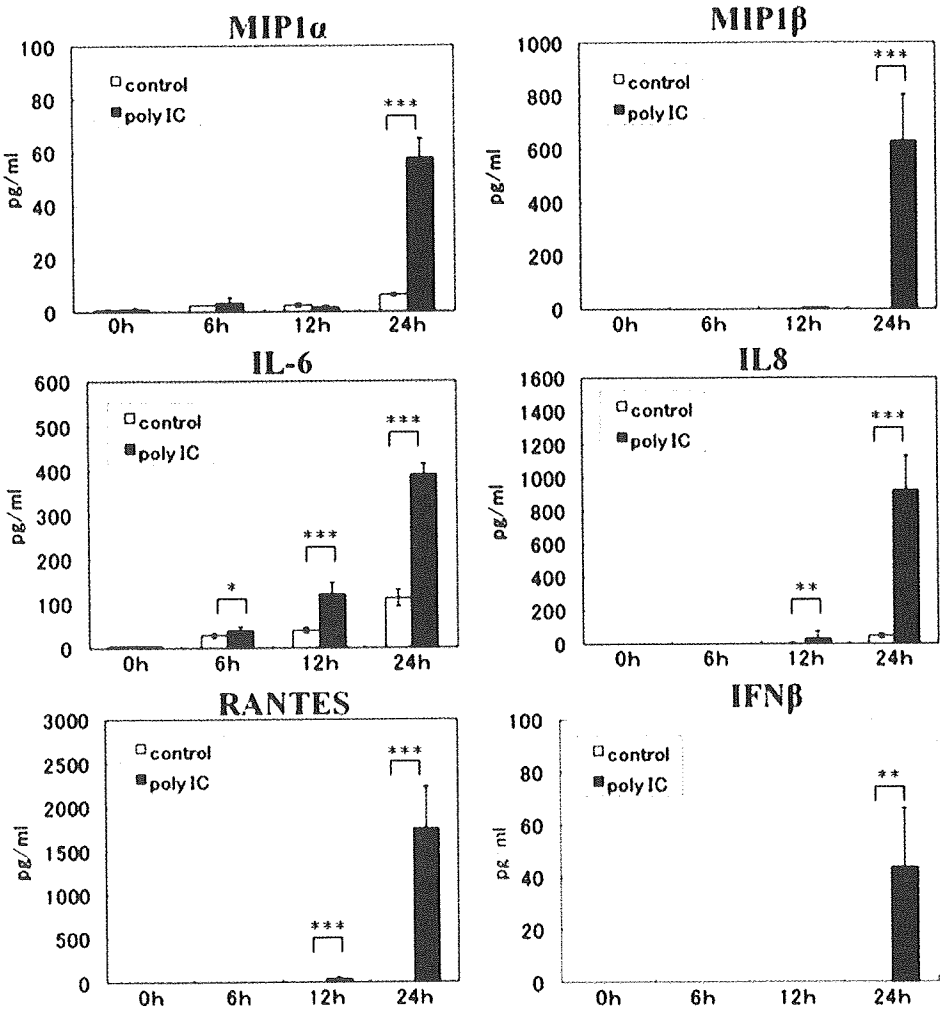

Figure 2. Cytokines and chemokines secreted by HCECs treated with poly(I:C). Culture medium was collected at 6, 12, and 24 h after poly(I:C) stimulation and analyzed for MIP1-α, MIP1-β, IL-6, IL-8, RANTES, and IFN-β protein by ELISA. The p values were calculated using two-tailed paired t-tests (*p<0.05, **p<0.01, ***p<0.001).

the participation of the TLR3 systems in signaling the HSV-1 infection on HCECs, the HCECs were pre-incubated with or without DEX, and then inoculated with HSV-1. To collect the cells before plaque formation, the time period from inoculation to testing was reduced to 24 h, and the inoculated dose increased to a MOI of 1,000, to allow detection of changes in inflammatory cytokines/chemokines. Therefore, HCECs were pre-incubated with or without DEX (10^{-5} M), followed by HSV-1 inoculation with a MOI of 1,000, and the cells collected for real-time PCR after 24 h.

Statistical analyses: Each experiment was repeated 3 times, and representative results are shown in the figures. Values are presented as means±standard deviations (SDs). Differences between the groups were determined by two-tailed paired t-tests. A p-value of <0.05 was considered to be statistically significant.

RESULTS

Poly(I:C)-induced TLR3 signaling pathway: To determine whether the TLR3/TRIF pathway is active in cultured HCECs, the HCECs were incubated with 100 ng/ml of poly(I:C) for 6, 12, and 24 h. Real time RT-PCR was then performed on the cells with primer pairs for *MIP1-α*, *MIP1-β*, *IL-6*, *IL-8*, *RANTES*, *IFN-β*, and *TLR3*. After stimulation by poly(I:C), the expression of the mRNA of *MIP1-α*, *IL-6*, *IL-8*, and *RANTES* were up-regulated as early as 6 h, and the level had increased 750 fold, 60 fold, 50 fold, and 10,000 fold, respectively, at 24 h. *MIP1-β* was also up-regulated at 12 h and reached about 400 fold at 24 h. *IFN-β* was up-regulated 9.9 fold within 6 h, which was maintained for 24 h (Figure 1). *TLR3* was also up-regulated at 12 h, and the level had increased about 40 fold after 24 h (Figure 2A). The expressions of inflammatory cytokines/chemokines and *TLR3* were not significantly altered without poly(I:C) stimulation (Figure 1 and Figure 2A).

The supernatants of the culture media were collected at 0, 6, 12, and 24 h, and the levels of MIP1-α, MIP1-β, IL-6, IL-8, RANTES, and IFN-β was evaluated using ELISA. The levels of MIP1-α, MIP1-β, and RANTES in the supernatant were elevated from undetectable levels at 0 h to 57.6 pg/ml,

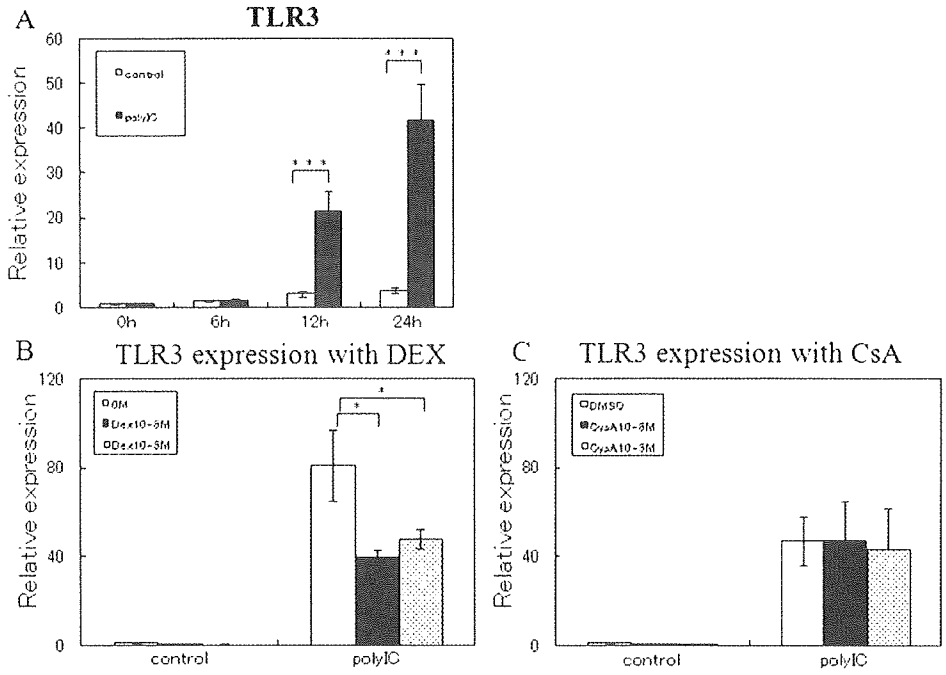

Figure 3. Effect of DEX and CsA on the expression of TLR3 by HCECs exposed to poly(I:C). Total RNA was isolated from HCECs at 6, 12, and 24 h after poly(I:C) stimulation (**A**), or from HCECs cultured with or without of DEX (**B**) or CsA (**C**) for 24 h and stimulated with poly(I:C) for 24 h. The expression of the mRNA of *TLR3* was determined by real-time PCR. The relative level of expression of each cytokine and chemokine mRNA is normalized against *G3PDH* mRNA expression. The p values were calculated using two-tailed paired t-tests (*p<0.05, **p<0.01, ***p<0.001).

630 pg/ml, and 1748.7 pg/ml, respectively, at 24 h after poly(I:C) stimulation. There was a slight but not significant elevation without poly(I:C) stimulation. The levels of IL-6 and IL-8 were slightly elevated without poly(I:C) stimulation, but were significantly elevated to 390 pg/ml and 920 pg/ml, respectively, at 24 h after poly(I:C) stimulation. The level of IFN-β was elevated to 43.8 pg/ml by poly(I:C) after 24 h, and no production of IFN-β was found without poly(I:C) stimulation (Figure 3).

Effect of DEX and CsA on TLR 3 signaling pathway: To determine whether DEX and CsA altered the expressions of the poly(I:C)-induced TLR3 and inflammatory cytokines/chemokines, HCECs were cultured with 100 ng/ml of poly(I:C) with or without DEX (10^{-6} or 10^{-5} M) or CsA (10^{-6} or 10^{-5} M). After 24 h, the cells and supernatants were collected, and the expression of the mRNAs and proteins of IL-6, IL-8, IFN-β, and TLR3 were evaluated by real-time PCR and ELISA.

Incubation with DEX down-regulated the poly(I:C)-induced expression of *TLR3* mRNA about 0.5 fold with 10^{-6} M and 0.6 fold with 10^{-5} M of DEX, whereas no effect was found when incubated with CsA (Figure 2B,C).

Incubation with DEX down-regulated the poly(I:C)-induced expression of the mRNA of *IL-6* about 0.4 fold with 10^{-6} M and 0.5 fold with 10^{-5} M of DEX (Figure 4). ELISA also showed that the poly(I:C) induced IL-6 production was decreased about 0.6 fold with 10^{-6} M and 0.5 fold with 10^{-5} M of DEX (Figure 5). The poly(I:C)-induced expressions of the mRNA and proteins of IL-8 were more significantly down-regulated by DEX, and the decrease was dose-dependent. Real-time PCR showed that the expression of the mRNA of *IL-8* was down-regulated about 0.4 fold with 10^{-6} M and 0.3 fold with 10^{-5} M of DEX. ELISA also showed a reduced production of IL-8 protein of about 0.5 fold with 10^{-6} M and 0.4 fold with 10^{-5} M of DEX (Figure 4 and Figure 5). DEX also down-regulated the poly(I:C)-induced mRNA expression of *IFN-β* by about 0.5 fold with 10^{-6} M and 10^{-5} M of DEX and decreased IFN-β production by about 0.6 fold with 10^{-6} M and 0.5 fold with 10^{-5} M of DEX (Figure 4 and Figure 5).

The effect of CsA on the poly(I:C)-induced inflammatory cytokine/chemokine expression was not as extensive as with DEX. However, the poly(I:C)-induced *IL-6* mRNA expression was down-regulated about 0.8 fold with 10^{-5} M of CsA, and ELISA showed that the poly(I:C) induced IL-6 production was reduced about 0.7 fold with 10^{-5} M of CsA (Figure 4 and Figure 5). The poly(I:C)-induced *IL-8* mRNA expression was also down-regulated about 0.65 fold with 10^{-5} M of CsA (Figure 4), and ELISA showed a decrease in production of about 0.65 fold with 10^{-5} M of CsA (Figure 5). Interestingly, CsA had no effect on poly(I:C)-induced *IFN-β* mRNA expression or production (Figure 4 and Figure 5).

Immunohistochemical staining for NFκB and IRF3: The effect of DEX (10^{-5} M) or CsA (10^{-5} M) on the activation of NFκB and IRF-3 was determined immunohistochemically after 3 h of stimulation by poly(I:C). NFκB p65 and IRF-3 staining were weakly detected in the cytosol of cultured HCECs without poly(I:C) stimulation (Figure 6A,E), but activated NFκB p65 and IRF-3 were clearly detected in the nuclei of most of cultured HCECs 3 h after stimulation by poly(I:C; Figure 6B,F). After stimulation by poly(I:C) in the presence of DEX, NFκB p65 and IRF-3 were detected in the nuclei of some HCECs but only in the cytosol of other HCECs

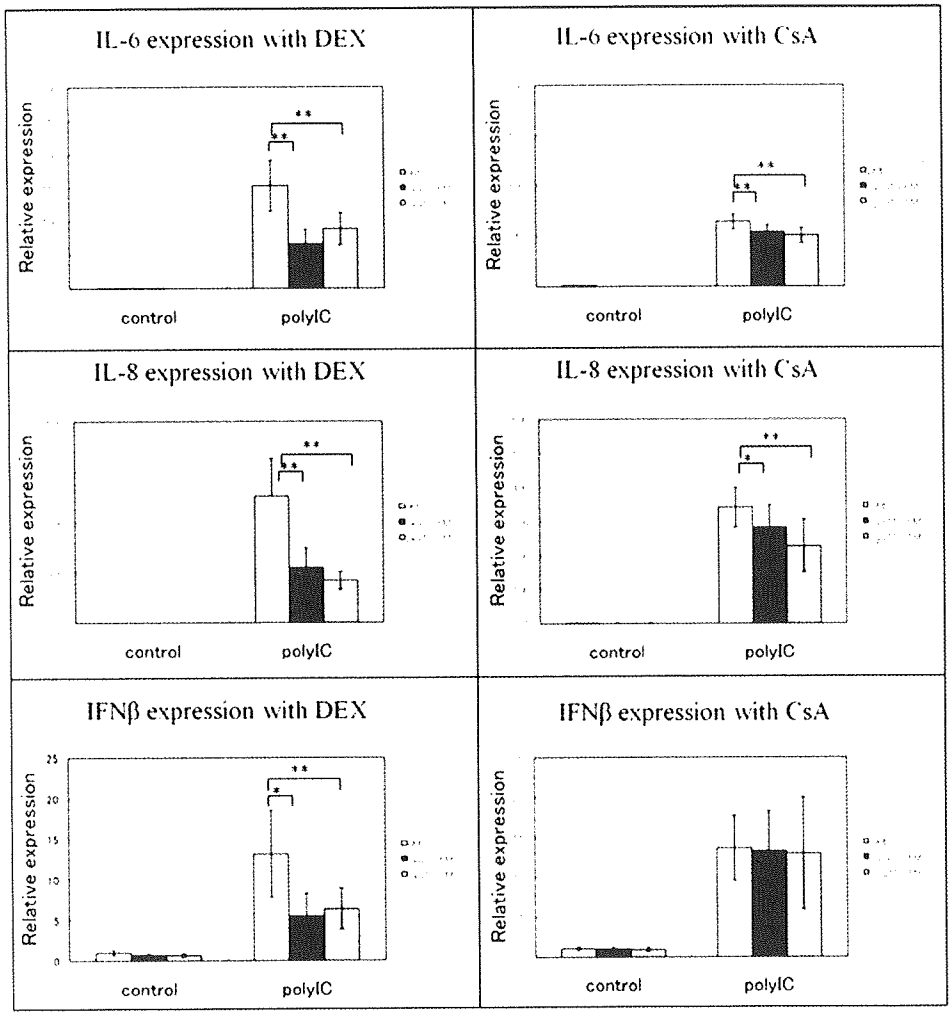

Figure 4. Effect of DEX and CsA on the expression of cytokines and chemokines by HCEs treated with poly(I:C). Total RNA was isolated from HCECs cultured with or without of DEX or CsA for 24 h and stimulated with poly(I:C) for 24 h. The expressions of the mRNAs of *IL-6*, *IL-8*, and *IFN-β* were determined by real-time PCR. The relative level of expression of each cytokine and chemokine mRNA is normalized to the level of *G3PDH* mRNA expression. The p values were calculated using two-tailed paired-tests (*p<0.05, **p<0.01, ***p<0.001).

(Figure 6C,G). After stimulation by poly(I:C), NFκB p65 staining was detected in more HCEC nuclei after exposure to CsA than to DEX, but some HCECs were stained only in the cytosol when exposed to CsA (Figure 6D). IRF3 was detected only in the nuclei of cultured HCECs after 3 h of stimulation by poly(I:C) in the presence of CsA (Figure 6H).

Effect of DEX and CsA on Herpes simplex virus 1 (HSV-1) infection: To determine whether DEX and CsA affected the HSV-1 infection of HCECs, HCECs were cultured in the presence or absence of DEX (10^{-5} M) or CsA (10^{-5} M), and inoculated with HSV-1 at a MOI of 50. The plaque area was increased when HCECs were pre-incubated with DEX, but CsA had no effect on HSV-1 infection (Figure 7A). Real time PCR showed more *HSV-1* DNA in the supernatant of DEX-exposed HCECs (Figure 7B).

In addition, we investigated the involvement of TLR3 signaling systems in HSV-1 infection of HCECs. Real-time PCR showed that the expressions of *IL6*, *IFN-β*, and *TLR3* were down-regulated by DEX when HCECs were inoculated with HSV-1 (Figure 8). *IL-6* and *IL-8* were also down-regulated, although the decrease was not statistically significant for *IL-8* (Figure 8).

DISCUSSION

Our results showed that poly(I:C), a TLR3 agonist, up-regulated the production of inflammatory cytokines/chemokines such as MIP1-α, MIP1-β, RANTES, IL-6, and IL-8, by activating NFκB. Incubation of HCECs with poly(I:C) also activated IRF3 followed by IFN-β production. The up-regulated expression of TLR 3 by poly(I:C) indicates that the TLR3/TRIF signaling pathways were most likely activated by poly(I:C) in HCECs. This is consistent with previous reports [1,15-17]. The cytokines and chemokines investigated are known to have powerful effects in recruiting immune cells and stimulating the maturation of dendritic cells [29-31]. Therefore, we suggest that corneal epithelial cells, when the TLR3s are activated de novo, are able to recruit and activate immune cells against viral infections.

Our results showed that DEX and CsA inhibit the poly(I:C)-induced NFκB activation and the subsequent

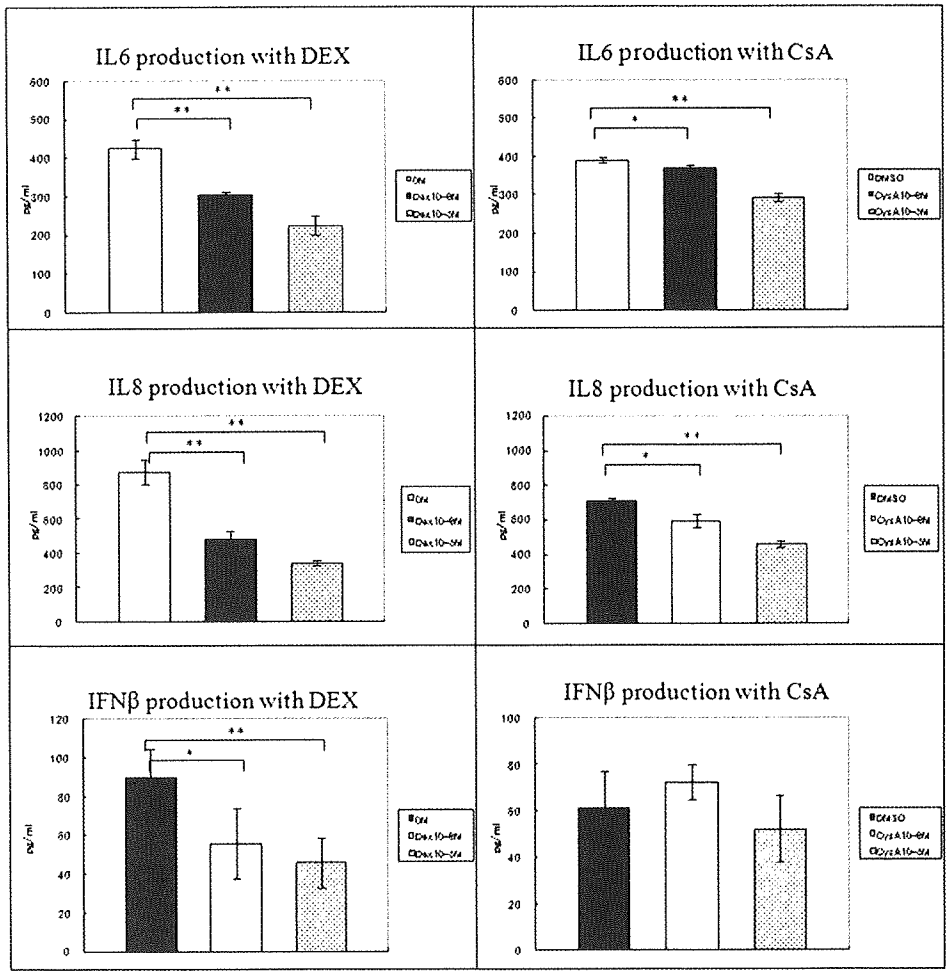

Figure 5. Cytokines and chemokines secreted by HCECs stimulated with poly(I:C) and cultured with or without DEX or CsA for 24 h. Culture medium was collected 24 hours after poly(I:C) stimulation and analyzed for the presence of IL-6, IL-8, and IFN-β protein by ELISA. The p values were calculated using two-tailed paired-tests, (*p<0.05, **p<0.01, ***p<0.001).

production of inflammatory cytokines/chemokines. Earlier studies have shown that the concentration of topically applied reagents in tears sharply decreases to less than 1/100 of the original concentration by one hour after administration, and keeps decreasing until only trace levels remain [32,33]. The concentrations of DEX and CsA used in this study were 1/500 and 1/5,000 of the concentration used in eye drops in a clinical setting (0.05%), and so the results should be clinically applicable.

Glucocorticoids, potent inhibitors of immune responses, act through glucocorticoid receptors (GRs) to depress the activities of other DNA-bound transcription factors, such as activator protein 1(AP-1) and NFκB [34-37]. CsA is known to inhibit T cell activation and proliferation [38]. Recent studies have shown that the inhibitory effects of CsA result from interference in the degradation of inhibitory kappaB (IκB) and a reduction in the transcriptional activity of the classic NFκB signaling pathway [39,40]. Our immunohistochemical results showed that DEX and CsA inhibit the poly(I:C)-induced nuclear translocation of NFκB, and these findings are in accord with earlier reports. Thus, the inhibition of inflammatory cytokines/chemokines by DEX and CsA in HCECs may result from the inhibition of NFκB, and this may be one of the mechanisms responsible for the immunosuppressive property of DEX and CsA.

DEX and CsA have different effects on the activation of IRF3 and IFN-β production, and both are part of the TRIF/TICAM-1 TLR3 signaling pathways [15,17,18]. DEX inhibited the poly(I:C)-induced IRF3 activation and the subsequent IFN-β production, while CsA inhibited neither IRF3 activation nor IFN-β production. The exact mechanism of action of DEX and CsA on IRF3 has still not been determined, however Reily et al. [41] have identified the glucocorticoid receptor-interacting protein 1 (GRIP1) to be an IRF3-interacting protein that facilitates IRF3-mediated transcription. They showed that the GRIP1:IRF3 interaction is blocked by the activation of GRs [41]. Our finding that DEX inhibited the poly(I:C)-induced IRF3 activation in HCECs is in accord with their findings.

The different effects of DEX and CsA on the activation of IRF3 and IFN-β production might also be explained by their differing effects on the expression of TLR3. Because the IFN-